AIR FORCE REPORT NO.
SAMSO-TR-72-123

AEROSPACE REPORT NO.
TR-0172(2230-20)-12

Properties of GaAs Schottky Barrier Mixers at 3. 3 mm

Prepared by R. D. ETCHEVERRY, W. A. JOHNSON, and T. T. MORI
Electronics Research Laboratory

72 MAY 30

Laboratory Operations
THE AEROSPACE CORPORATION

Prepared for SPACE AND MISSILE SYSTEMS ORGANIZATION
AIR FORCE SYSTEMS COMMAND
LOS ANGELES AIR FORCE STATION
Los Angeles, California

LABORATORY OPERATIONS

The Laboratory Operations of The Aerospace Corporation is conducting experimental and theoretical investigations necessary for the evaluation and application of scientific advances to new military concepts and systems. Versatility and flexibility have been developed to a high degree by the laboratory personnel in dealing with the many problems encountered in the nation's rapidly developing space and missile systems. Expertise in the latest scientific developments is vital to the accomplishment of tasks related to these problems. The laboratories that contribute to this research are:

Aerodynamics and Propulsion Research Laboratory: Launch and reentry aerodynamics, heat transfer, reentry physics, propulsion, high-temperature chemistry and chemical kinetics, structural mechanics, flight dynamics, atmospheric pollution, and high-power gas lasers.

Electronics Research Laboratory: Generation, transmission, detection, and processing of electromagnetic radiation in the terrestrial and space environments, with emphasis on the millimeter-wave, infrared, and visible portions of the spectrum; design and fabrication of antennas, complex optical systems, and photolithographic solid-state devices; test and development of practical superconducting detectors and laser devices and technology, including high-power lasers, atmospheric pollution, and biomedical problems.

Materials Sciences Laboratory: Development of new materials; metal matrix composites and new forms of carbon; test and evaluation of graphite and ceramics in reentry; spacecraft materials and components in radiation and high-vacuum environments; application of fracture mechanics to stress corrosion and fatigue-induced fractures in structural metals; effect of nature of material surfaces on lubrication, photosensitization, and catalytic reactions, and development of prosthesis devices.

Plasma Research Laboratory: Reentry physics and nuclear weapons effects; the interaction of antennas with reentry plasma sheaths; experimentation with thermonuclear plasmas; the generation and propagation of plasma waves in the magnetosphere; chemical reactions of vibrationally excited species in rocket plumes; and high-precision laser ranging.

Space Physics Laboratory: Aeronomy, density and composition of the atmosphere at all altitudes, atmospheric reactions and atmospheric optics; pollution of the environment, the sun, earth's resources; meteorological measurements; radiation belts and cosmic rays, and the effects of nuclear explosions, magnetic storms, and solar radiation on the atmosphere.

THE AEROSPACE CORPORATION
El Segundo, California

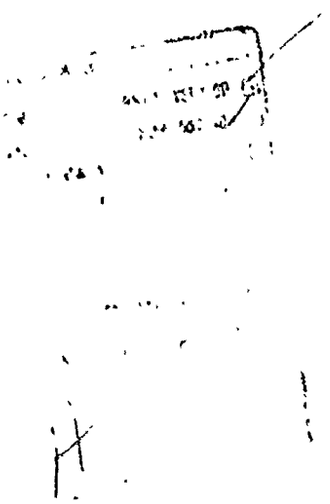

UNCLASSIFIED
Security Classification

DOCUMENT CONTROL DATA - R & D
(Security classification of title, body of abstract and indexing annotation must be entered when the overall report is classified)

1. ORIGINATING ACTIVITY (Corporate author) The Aerospace Corporation El Segundo, California	2a REPORT SECURITY CLASSIFICATION Unclassified 2b GROUP

3. REPORT TITLE
Properties of GaAs Schottky Barrier Mixers at 3.3 mm

4 DESCRIPTIVE NOTES (Type of report and inclusive dates)

5 AUTHOR(S) (First name, middle initial, last name)
Robert D. Etcheverry, Walter A. Johnson, and Tsutomu T. Mori

6 REPORT DATE	7a TOTAL NO. OF PAGES	7b NO. OF REFS
72 MAY 30	57	29

8a CONTRACT OR GRANT NO.	9a ORIGINATOR'S REPORT NUMBER(S)
F04701-71-C-0172 b PROJECT NO.	TR-0172(2230-20)-12
c d	9b OTHER REPORT NO(S) (Any other numbers that may be assigned this report) SAMSO-TR-72-123

10. DISTRIBUTION STATEMENT
Approved for public release; distribution unlimited.

11. SUPPLEMENTARY NOTES	12. SPONSORING MILITARY ACTIVITY
	Space and Missile Systems Organization Air Force Systems Command United States Air Force

13 ABSTRACT
Design and performance data are given for a 3.3-mm broadband mixer employing GaAs Schottky barrier diodes. Included are conversion loss and noise temperature ratio measurements on a series of mixers. Both single-ended and balanced configurations are considered.

Ta

DD FORM 1473

UNCLASSIFIED
Security Classification

14

KEY WORDS

Excess noise ratio
Millimeter waves
Schottky barrier mixer

Distribution Statement (Continued)

Abstract (Continued)

Air Force Report No.
SAMSO-TR-72-123

Aerospace Report No.
TR-0172(2230-20)-12

PROPERTIES OF GaAs SCHOTTKY BARRIER MIXERS AT 3.3 mm

Prepared by

R. D. Etcheverry, W. A. Johnson, and T. T. Mori
Electronics Research Laboratory

72 MAY 30

Laboratory Operations
THE AEROSPACE CORPORATION

Prepared for

SPACE AND MISSILE SYSTEMS ORGANIZATION
AIR FORCE SYSTEMS COMMAND
LOS ANGELES AIR FORCE STATION
Los Angeles, California

IC

FOREWORD

This report is published by The Aerospace Corporation, El Segundo, California, under Air Force Contract No. F04701-71-C-0172.

This report, which documents research carried out from June 1969 through June 1970, was submitted on 20 March 1972 to Lieutenant William E. Belote, SYAE, for review and approval.

The authors wish to thank the many members of the staff of the Electronics Research Laboratory who aided in this research. Particular thanks are due to G. Berry, who fabricated the mounts and contributed greatly to their mechanical design, and Drs. M. Millea and M. McColl, who devised the copper doping technique and furnished us with the processed material.

Approved

A. H. Silver, Director
Electronics Research Laboratory

Publication of this report does not constitute Air Force approval of the report's findings or conclusions. It is published only for the exchange and stimulation of ideas.

W. E. Belote
Lieutenant, United States Air Force
Project Officer

ABSTRACT

Design and performance data are given for a 3.3-mm broadband mixer employing GaAs Schottky barrier diodes. Included are conversion loss and noise temperature ratio measurements on a series of mixers. Both single-ended and balanced configurations are considered.

CONTENTS

Preceding page blank

FIGURES

FIGURES (Continued)

I. INTRODUCTION

With the advent of solid state sources with sufficient power to serve as local oscillators and perhaps eventually as useful transmitters there has been greatly increased interest in millimeter wave communications systems. With the exception of a few experimental devices (Refs. 1 and 2), there are no low noise amplifying devices available below about 8 mm; therefore millimeter mixers assume a role of paramount importance in receiver design. Although there have been a number of papers (Refs. 3-18) describing millimeter mixers using both point contact and Schottky barrier diodes, there is generally a lack of information concerning both the band-shape characteristics and the noise temperature ratios of millimeter mixers. This paper provides these data for a number of our 3.3-mm mixers.

The characteristics of the 3-μm-diam GaAs Schottky barrier diodes used in our mixers differ somewhat from those ordinarily expected (Ref. 19) for a metal contact on the original material. These differences result from the addition of Cu impurity in the GaAs. In this process a 2000-Å-thick, high-resistivity region is produced on heavily doped n-type GaAs. An extended space charge region is formed that changes the electric field profile in the semiconductor so as to reduce the capacitance of the diode by a factor of between 5 and 10. Nickel and gold plating on the GaAs forms the Schottky barrier.

These diodes are then placed in mounts similar to the Adtec Corporation mount described by Wentworth et al. (Ref. 20) and in an improved mount of our own design. The details of the construction of our mount are described in Section II, and the conversion performance of mixers in both types of mounts is given in Section III.

In any system in which the diode noise is comparable to the noise generated by the intermediate frequency (IF) amplifier following the mixer, the diode noise becomes as important to system performance as is mixer conversion. For this reason we made an extensive series of noise ratio

measurements on our diodes. The addition of the Cu impurity in the processing of the GaAs resulted in an unusual diode noise behavior. The measurement methods and results are presented in Section IV.

Noise figure measurements were made on various receivers with these mixers. The technique employed was the familiar hot-cold body method, for which we used a He-Ne gas tube calibrated against a precision liquid nitrogen standard with a Dicke radiometer. The results of these measurements are discussed in Section V.

II. DESIGN OF IMPROVED MIXER MOUNT

The Adtec mount with a point contact GaAs diode is capable of excellent broadband performance (Ref. 21). However, the lack of mechanical rigidity in the mount and the extremely delicate diode junction made use of the mount difficult even with the most careful laboratory handling.

This laboratory redesigned the mount in order to improve both the mechanical and electrical properties of the mixer. At the same time, we begin to fabricate GaAs Schottky barrier diodes.

One of the features of the point contact junction that contributed both to its excellent performance and to its fragility was the very small area of contact at the junction, which minimized junction capacity, thereby improving the RF matching of the diode. Any junction that did not have a very small junction contact area would match poorly, with a resultant high conversion loss. Even with Schottky barrier diameters of between 2 and 5 μm, we had a similar matching problem at 3.3 mm due to junction capacity. One possible broadband solution to this problem is reduction of the waveguide impedance level through reduction of the waveguide height. Since our waveguide heights are generally either 0.050 in. (WR-10) or 0.061 in. (WR-12), this is not a very attractive solution because of the very small mechanical tolerances involved. We found a better solution by changing the characteristics of the semiconductor material, as explained in the Introduction, thereby allowing the use of a standard guide without any sacrifice in the matching characteristics of the junction. With the RF matching problem alleviated by the semiconductor processing, it remained for us to make the structure of the mount more rugged.

Figures 1-3 show the mount design we used. We removed the long differential screw drive arrangement for the diode and the bulky N-type connector and the quarter-wave matching transformer. These two major changes considerably improved the mechanical rigidity. Additional rigidity

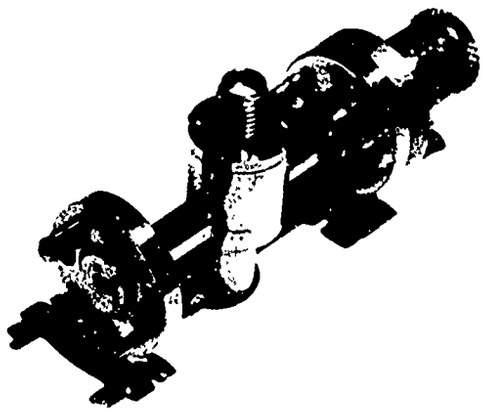

a. Assembled View

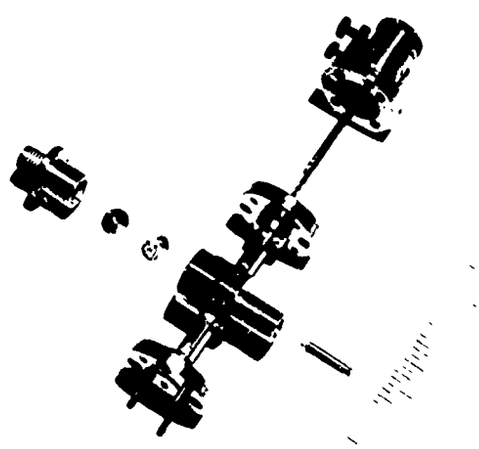

b. Disassembled View

Figure 1. The 94-GHz Diode Mount

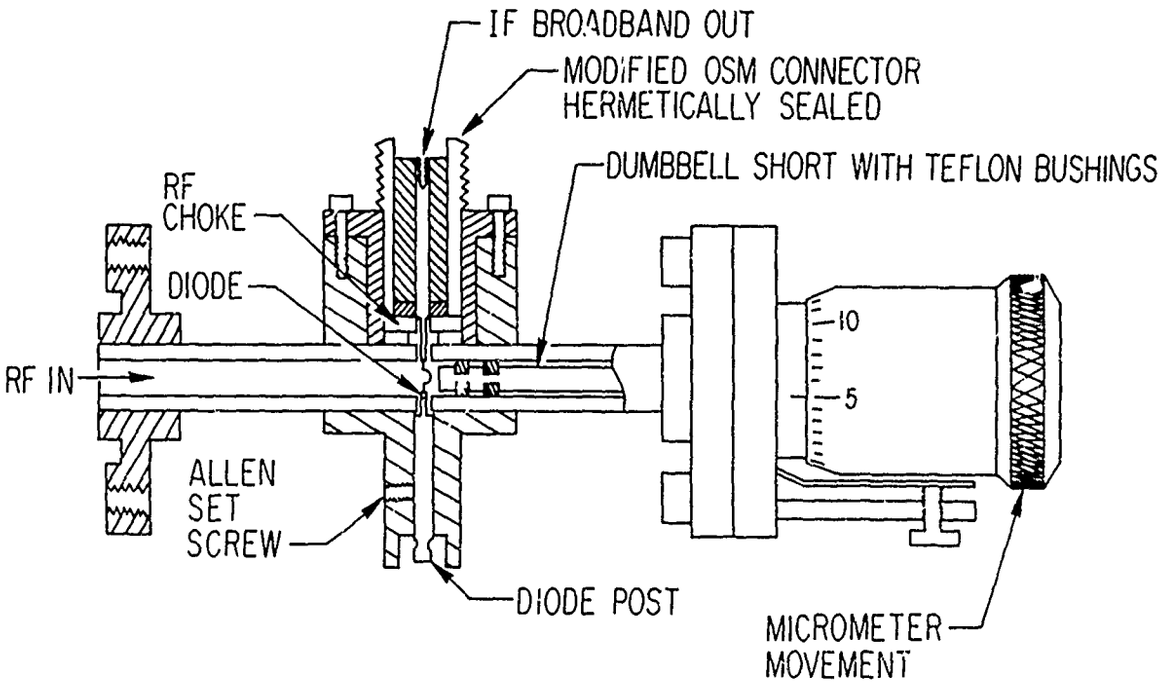

Figure 2. Cutaway View of the 94-GHz Diode Mount

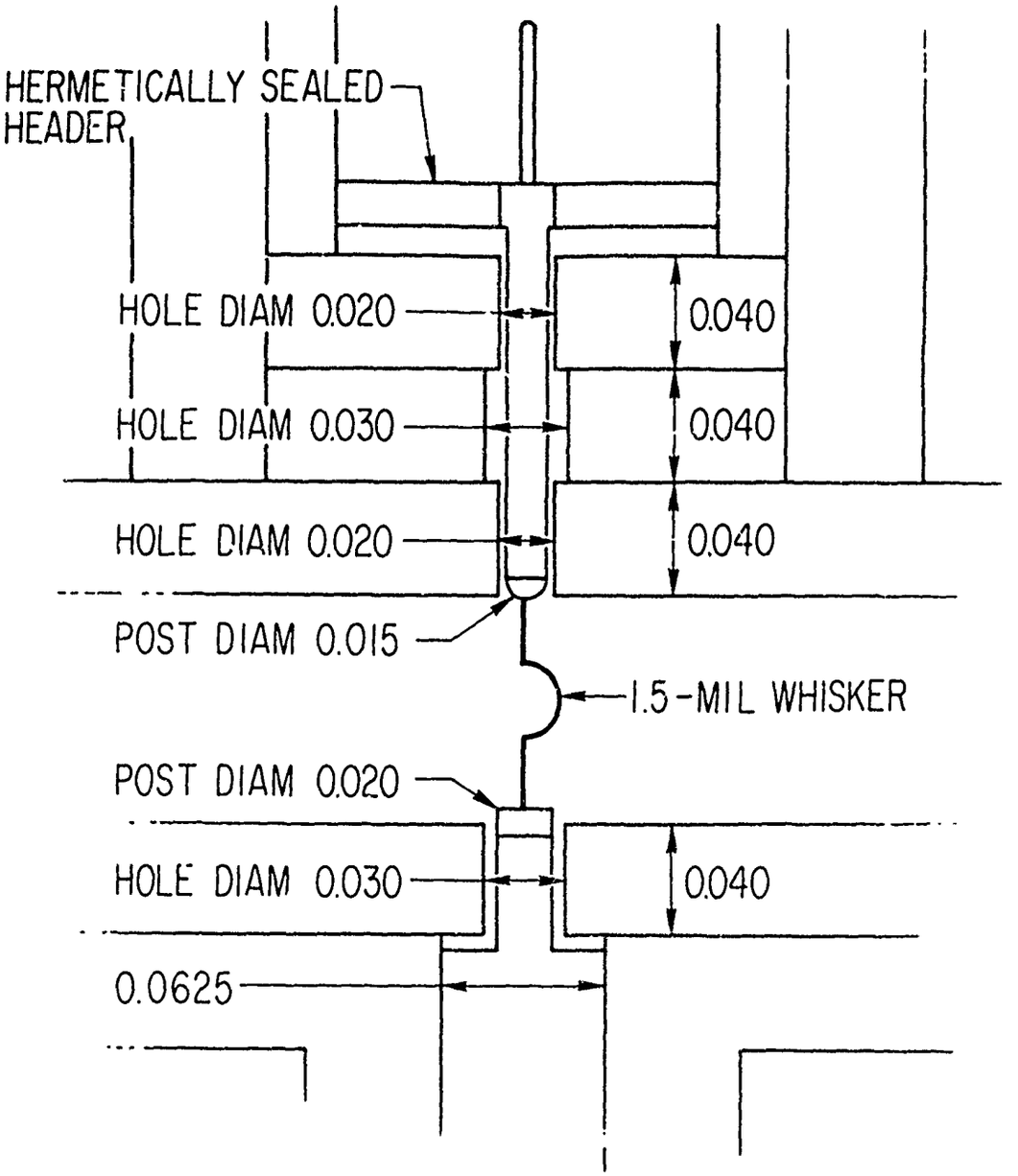

Figure 3. Central Portion of the 94-GHz Diode Mount

was obtained by the use of a modified OSM connector with a glass-to-metal seal. The hermetic seal prevents the center conductor from moving vertically and laterally in the mount. In the older mount design the center conductor would sometimes move and break the diode. The hermetically sealed OSM connector solved this problem entirely without any sacrifice of the IF bandwidth characteristics.

The whisker is made of annealed Au alloy wire of 0.0015-in. diam. It has a half-loop bend along its length to provide axial contact pressure against the Schottky diode dots on the GaAs material. We hand-form the whisker while viewing under a microscope. The radius of the half-loop is approximately 0.01 in. Pointing of the whisker is done electrolytically, and the method used is the same as that described in Ref. 22. The whisker is cut so that two conditions are met; the half-loop position is mid-positioned within the waveguide, and the whisker post plus solder are flush and do not protrude into the upper waveguide wall.

The brass rivet rod entrance into the waveguide wall is a tapered fit, primarily for mechanical reasons but also because it reduces RF leakage at the joint. It has been our expression that the best mixer performance occurs with the half-loop of the cat whisker across the waveguide.

We make the contact to the diode by manually advancing the diode post while observing the voltage vs forward current curve with a Tektronix Type 575 transistor curve tracer. When a stable diode curve is observed, the advancement is stopped. Contact pressure is then finally adjusted for optimum performance during measurements of either conversion loss or noise figure. The Allen screw is then set to hold the post securely. Since the function of the whisker-to-diode metalization contact is to provide ohmic contact and not actual diode formation, the whisker pressure is of much less importance than in the case of the point contact diode. We estimate our contact pressures to be several times greater than those of the point contact diodes. This is very important not only for reliability but also for simplicity.

An inverted-dumbbell type of structure is used to block the RF energy from propagating up the mixer IF output coaxial line. The RF choke consists

of quarter-wave spacings of alternate low- and high-impedance coaxial sections. As shown in Figure 3, these sections are formed by the waveguide wall and two small washers. The nominal inside diameters of the washers are 0.030 and 0.020 in. The OSM coaxial pin is 0.015 in. in diameter. This combination compromises between a low coaxial line Z_o impedance and effective low capacity for the IF rolloff point and provides an IF (3dB) cutoff of ~5 GHz, resulting in effective RF choking over a bandwidth of ~10 GHz.

The leakage fields in the vicinity of the mixer and its associated cables and connectors were probed with a small horn. So that a level on these leakage fields could be determined, the mixer assembly was removed and an identical small horn was attached to the waveguide. The field was again probed, and the resulting measured power level was 50-70 dB above the previously measured leakage fields.

Both positive and negative output diode mounts have been made. The GaAs diode chip is interchanged with the whisker to produce a mount with polarity opposite that of the mount shown in Figure 1.

III. MIXER CONVERSION PERFORMANCE

A block diagram of the test equipment configuration used to measure conversion loss is shown in Figure 4. Over the 85-95 GHz range, the backward wave oscillator (BWO) was leveled to ±0.5 dB at worst but generally was closer to ±0.25 dB. Our primary millimeter power standard was a TRG Model 980 water calorimeter. Three such instruments all agreed within narrow limits. Power calibrations below 40 GHz were made with a Hewlett Packard 431 Power Meter. We estimate the total error in these measurements to be, conservatively, less than ±1.0 dB and probably generally less than ±0.5 dB. VSWR measurements at RF were made with an FXR Model E103A slotted section and at IF with an HP8410A network analyzer.

The results of sweeps of various mounts are shown in Figures 5-11. In the figures the mount numbers prefixed with a "W" are our mounts (i.e , as shown in Figure 1) with W-band waveguide (WR-10). The mounts without the "W" prefix are Adtec-type mounts in E-band waveguide (WR-12). For these tests we used a total of 26 mounts, 11 of our design and 15 of the Adtec type. Approximately one-third of the mounts performed well, one-third were average, and one-third poor. Performance also varied considerably between runs of Schottky barrier material. The performance data given in this paper are for those mounts that gave the best results.

Figure 5 is a sweep of those mounts with the local oscillator (L.O.) at 90 GHz. A signal power reference (i.e., signal power into the mixer) curve taken with a well padded bolometer, also shown in Figure 5, shows how well the bolometers track each other; since we expect each of them to vary smoothly, we can infer that the leveled output of the BWO is a smooth function of the form shown in Figure 5. The bias tee (a Microlab HW-30N designed for 2-4 GHz) used for these sweeps had a low frequency cutoff of ~0.5 GHz. Unless otherwise noted, this was the bias tee used for all of the data presented. The periodic nature of the responses of mounts No. 9 and No. 11 is probably due to mismatches within the structure or perhaps a periodicity in the basic

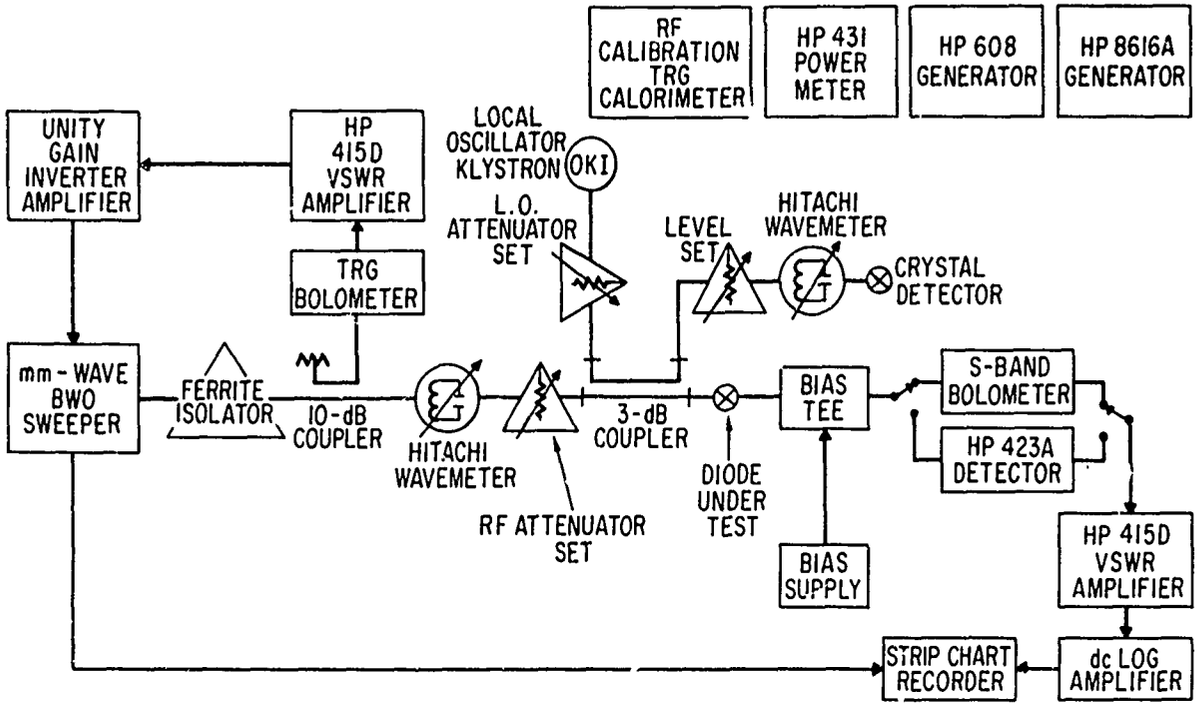

Figure 4. Swept Frequency Conversion Loss Test Setup

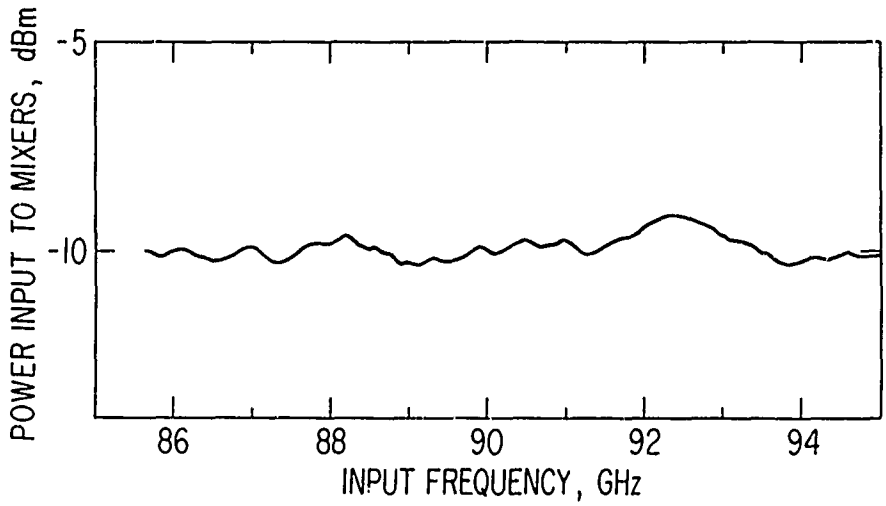

a. Power Input to Mixer

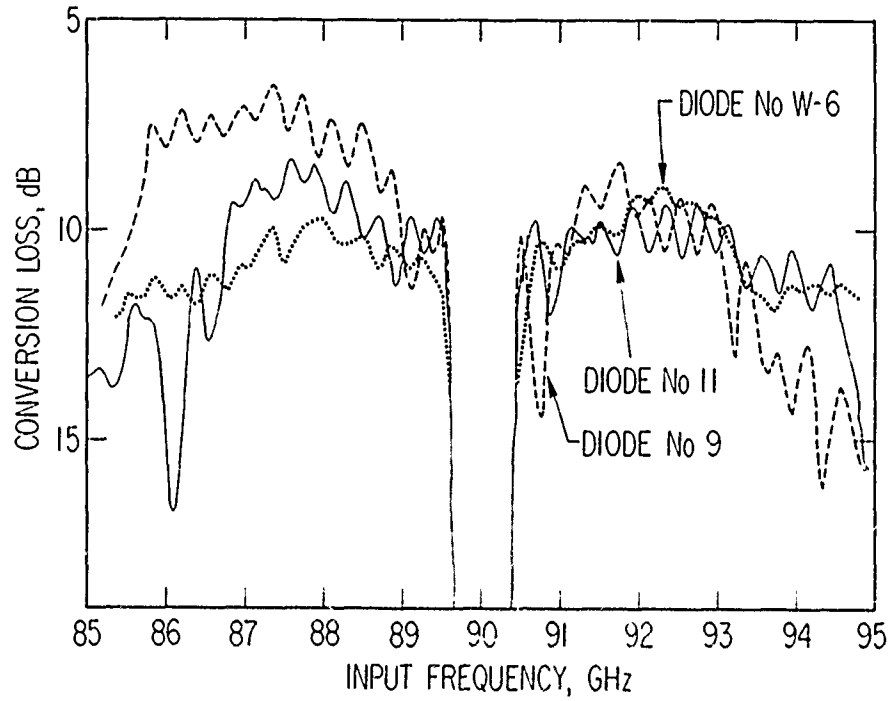

b. Swept Conversion Loss

Figure 5. Power Input to Mixer and Swept Conversion Loss vs Input Frequency for Diodes 9, 11, and W-6

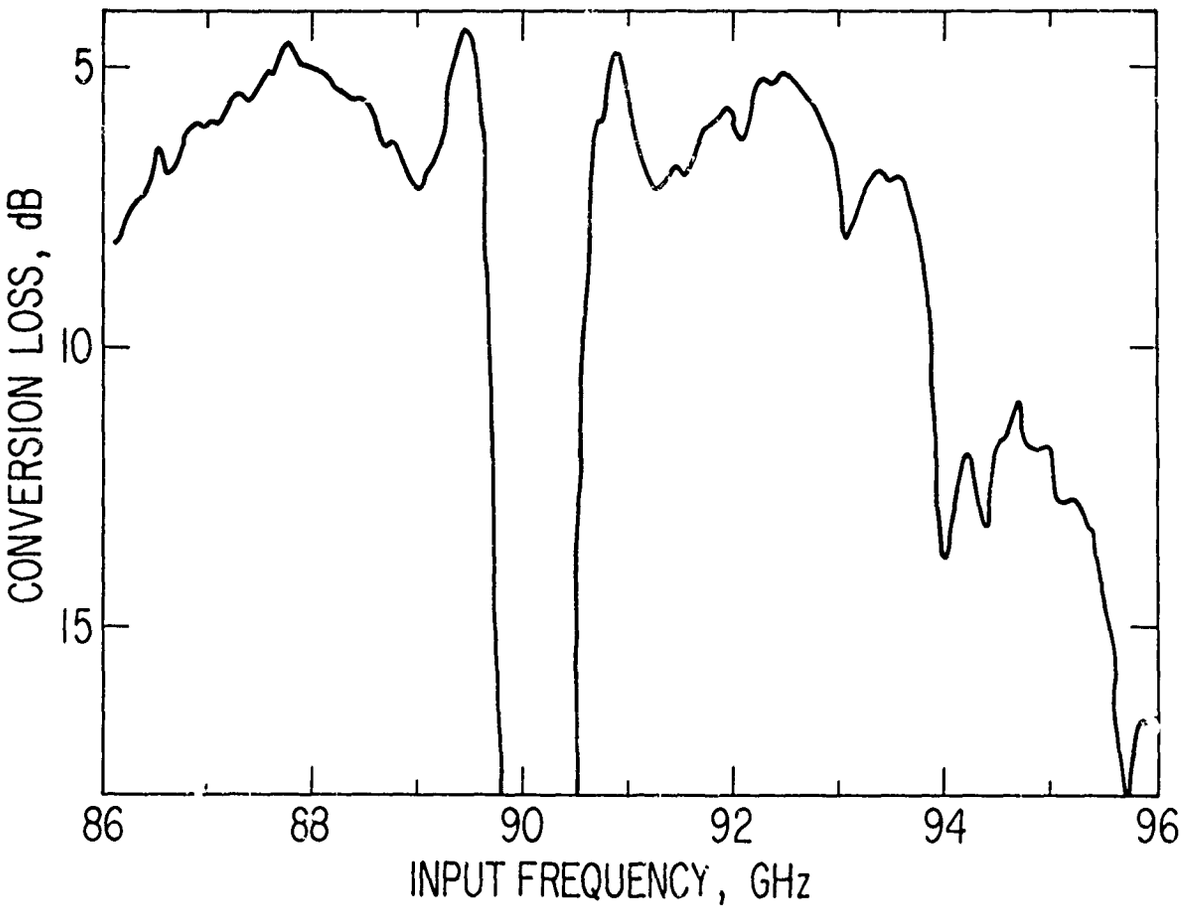

Figure 6. Swept Conversion Loss vs Input Frequency for Diode 13

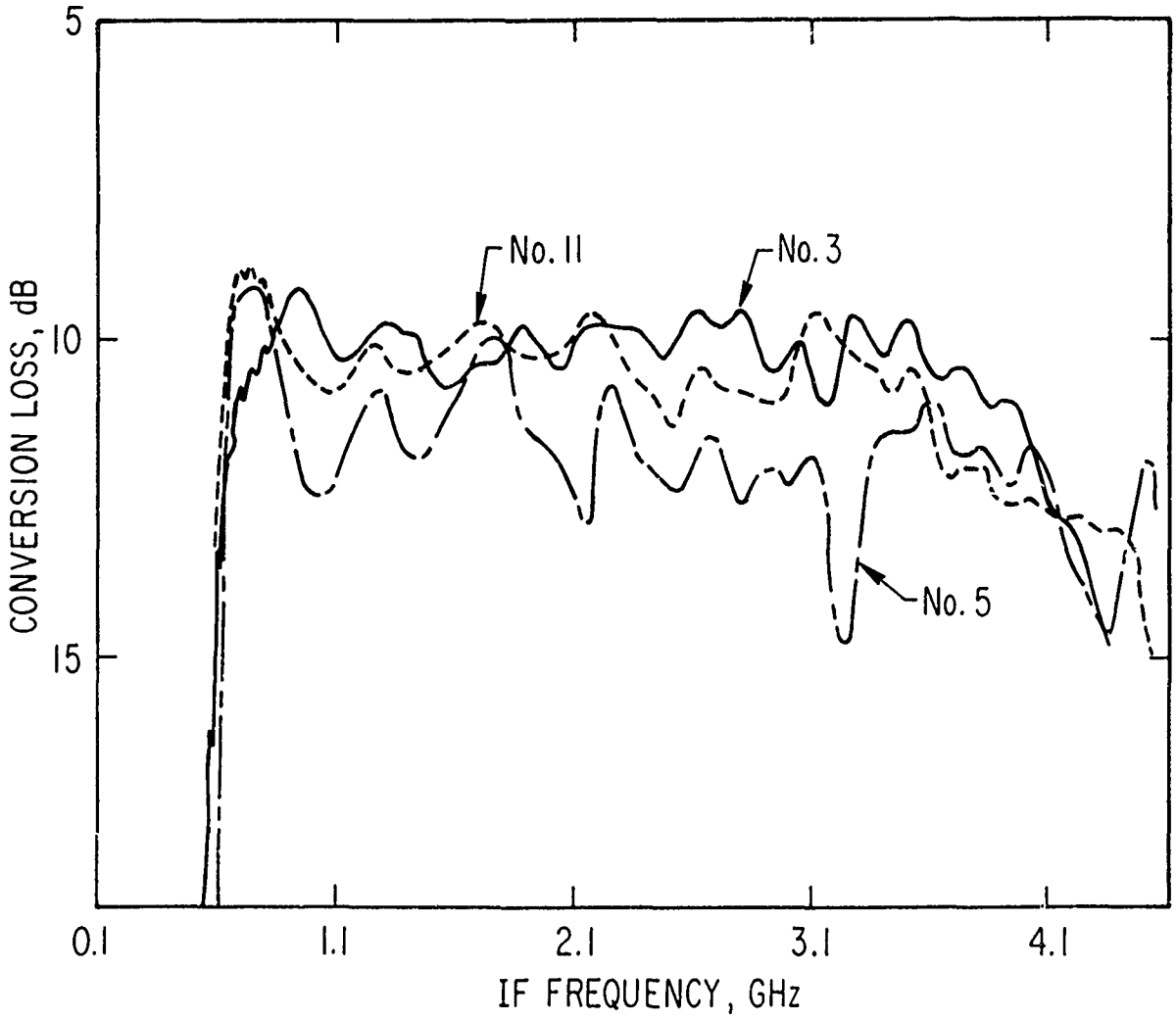

Figure 7. Swept Conversion Loss vs Input Frequency for Diodes 5, 11, and 3

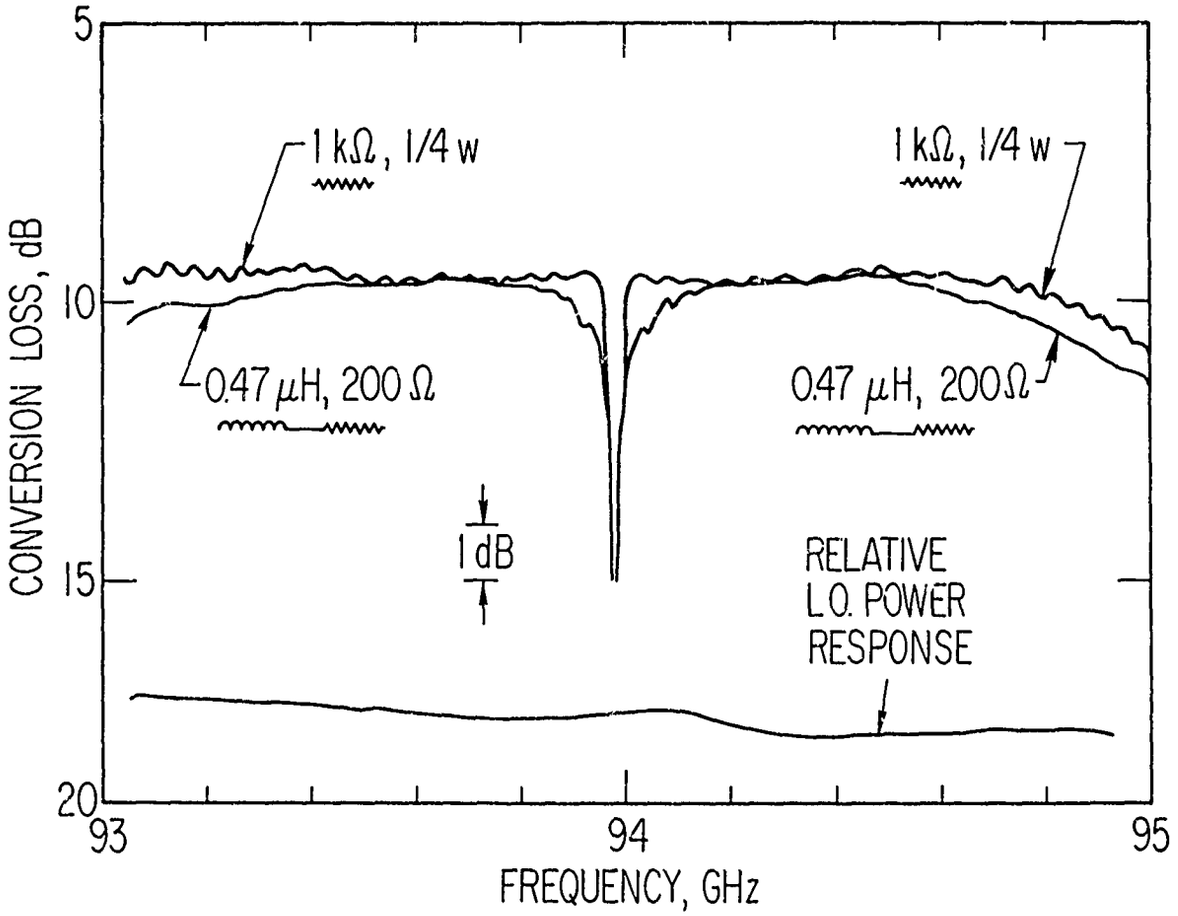

Figure 8. Swept Conversion Loss vs Frequency and Effects of Biasing Network for Diode W-6

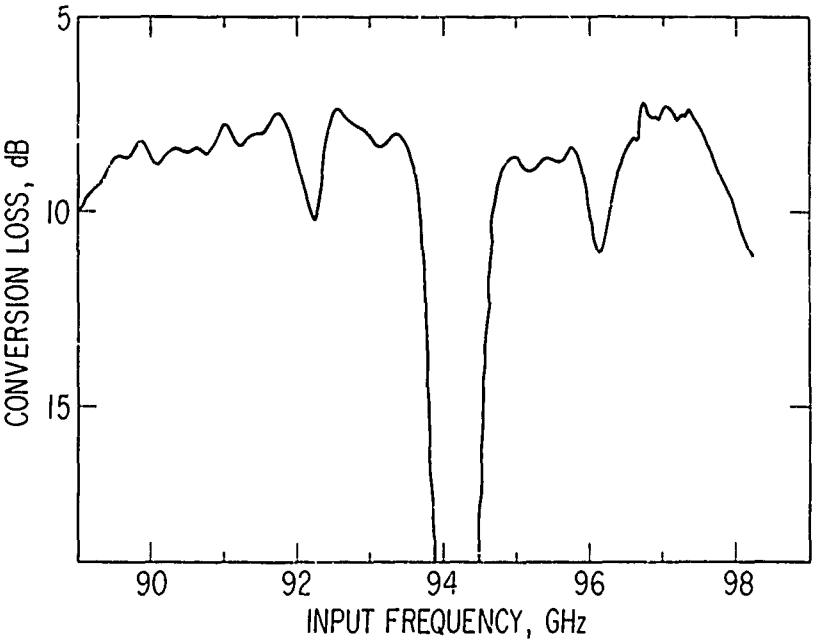

a. Uncorrected

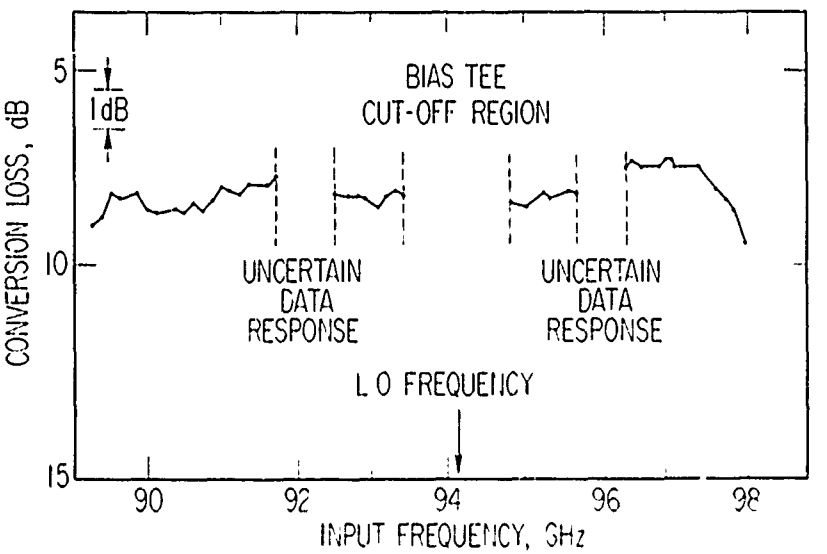

b. Corrected for Sweep Power Variations

Figure 9. Swept Conversion Loss vs Input Frequency for Diode W-5

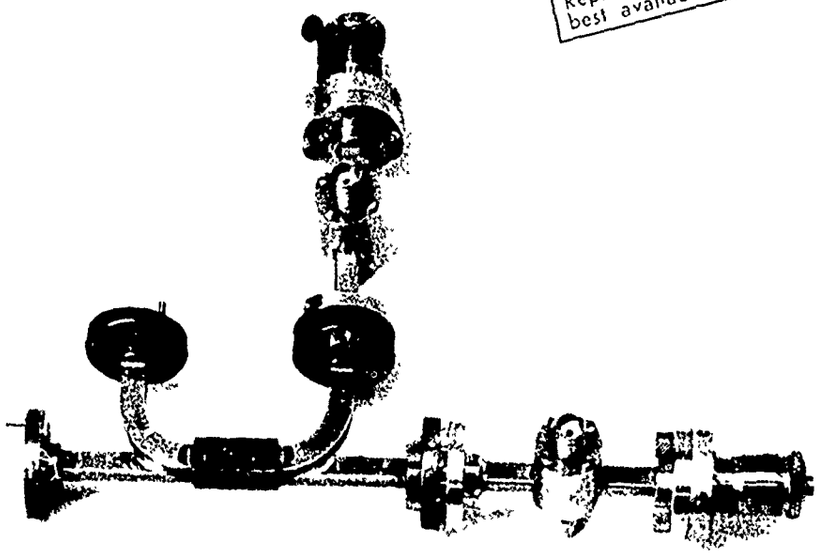

Figure 10. Balanced Mixer Configuration with 3-dB Hybrid Coupler

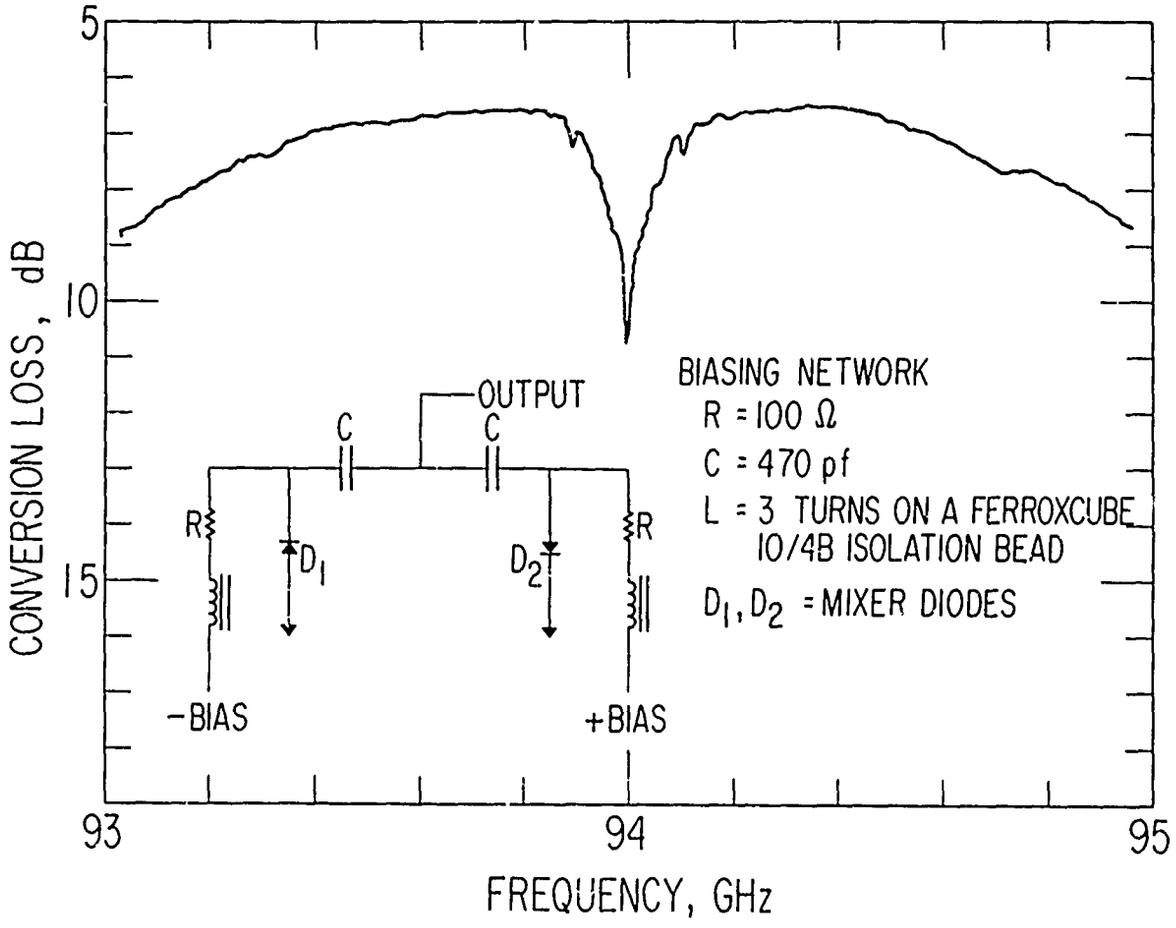

Figure 11. Swept Conversion Loss vs Frequency of Balanced Mixer Pair W-1 and W-2

frequency conversion process of the diode. It is not attributable to a simple mismatch problem at the RF input, since we know that our signal source VSWR (as measured at the output port of the 3-dB coupler in Figure 4) is generally less than 1.3:1. Mixer performance from the L.O. frequency to ±1 GHz or perhaps even ±1.5 GHz is somewhat masked by the bias tee response and the resonances (e.g., at 90.75 GHz in No. 9) between the tee and the mixer. The lowest conversion (6.5 dB) of the three is exhibited by No. 9 and the flattest performance (~10 GHz for ±1.5 dB) by W-6.

Figure 6 is a sweep of the mixer with the lowest conversion loss (4.5 dB. The response dips at 91.3 and 89.0 are caused by a broad resonance between the mixer IF structure and the bias tee.

Figure 7 is an expanded sweep of the upper sideband of three mounts with the L.O. at 90 GHz. Mounts No. 3 and No. 11 are flat within ±1.5 dB to 3.5 GHz. Mount No. 5, which is not as flat as No. 3 or No. 11 but converts almost as well over narrow bands, exhibits a noticeable periodicity as well as a resonant null at 3.25 GHz and possibly a resonant null at 2.15 GHz. The data shown for mount No. 11 in Figures 5 and 7 were taken some days apart. It is probable that the mixer changed characteristics slightly, which would account for the slight differences between Figures 5 and 7.

Figure 8 illustrates some of the problems associated with the biasing network. The narrowband (±1 GHz) conversion of mount W-6 was measured for two simple bias networks of our own design. The behavior close to the L.O. frequency at 93.9 GHz was about as we expected. We did not, however, expect the periodicity with the 1-kΩ biasing resistor, nor did we expect the 1-kΩ resistor to outperform the series combination of 200Ω and 0.47 μh above a 500-MHz IF. We have found that pure resistive biasing gives the best results for IF frequencies below 1 GHz, although a series combination of a resistor and a choke may also prove acceptable. Above 1 GHz, biasing through a choke (e.g., as in the Microlab HN-30N bias tee) gives the best results. When using choke biasing, we prefer a low-impedance source for the bias current, which allows us to use the rectified mixer current for tuning as well as to indicate how hard we are driving the diode.

Figure 9 shows a sweep of mount W-5 for an L.O. frequency of 94.2 GHz. Also shown is a corrected conversion curve, which is the result of point-by-point computation of conversion from power measurements made at RF with a TRG calorimeter and at IF with an HP power meter, as explained previously. Resonances between the mixer and the bias tee resulted in the dips between 91.75 and 92.55 GHz and between 95.85 and 96.55 GHz. Since it would be meaningless, we have not corrected these ranges and similarly have not corrected the range of bias-tee cutoff. The result is a corrected conversion that varies ±0.7 dB from 89.4 to 98.0 GHz.

Figure 10 shows two mounts with a 3-dB hybrid coupler in a balanced mixer configuration designed for use in our 3.2-mm radar receiver (Refs. 23-25) which necessitated excellent balance while requiring good conversion performance. The conversion performance is shown in Fig. 11. At the IF frequency of importance (400 MHz) the conversion is 6.5 dB on the upper sideband and 6.7 dB on the lower. The L.O. suppression curve, calculated by the method of Ref. 26, is shown in Figure 12. The suppression for the upper sideband was about 38 dB.

A plot of conversion loss vs local oscillator power is shown in Figure 13 for two mixers. We obtain the lowest conversion loss by first lightly biasing the diode with dc (~100 μA) and then driving the diode with between zero and +3 dBm. When a low-impedance bias source is used, the total current (bias plus rectified) for this condition is 1-4 mA. The same conversion performance is obtained with either high- or low-impedance biasing sources.

Table I lists the RF VSWR for a pair of diodes in the improved mount. Diodes mounted in the E-band Adtec mount generally exhibited slightly higher RF VSWR's. Over a 4-GHz input frequency range, the VSWR is less than 2.3:1 and is generally less than 2.0:1. Figure 14 plots the IF impedance of 10 mounts, all optimized for best conversion, with a local oscillator frequency of 94 GHz and an IF frequency of 125 MHz. The VSWR varies from 1.9:1 to 4.2:1, corresponding to mismatch losses of 0.38 and 2.08 dB, respectively. Typical performance without RF drive is shown in Figure 15 for mount No. 3 as a function of bias and IF frequency. For a given total diode current and IF

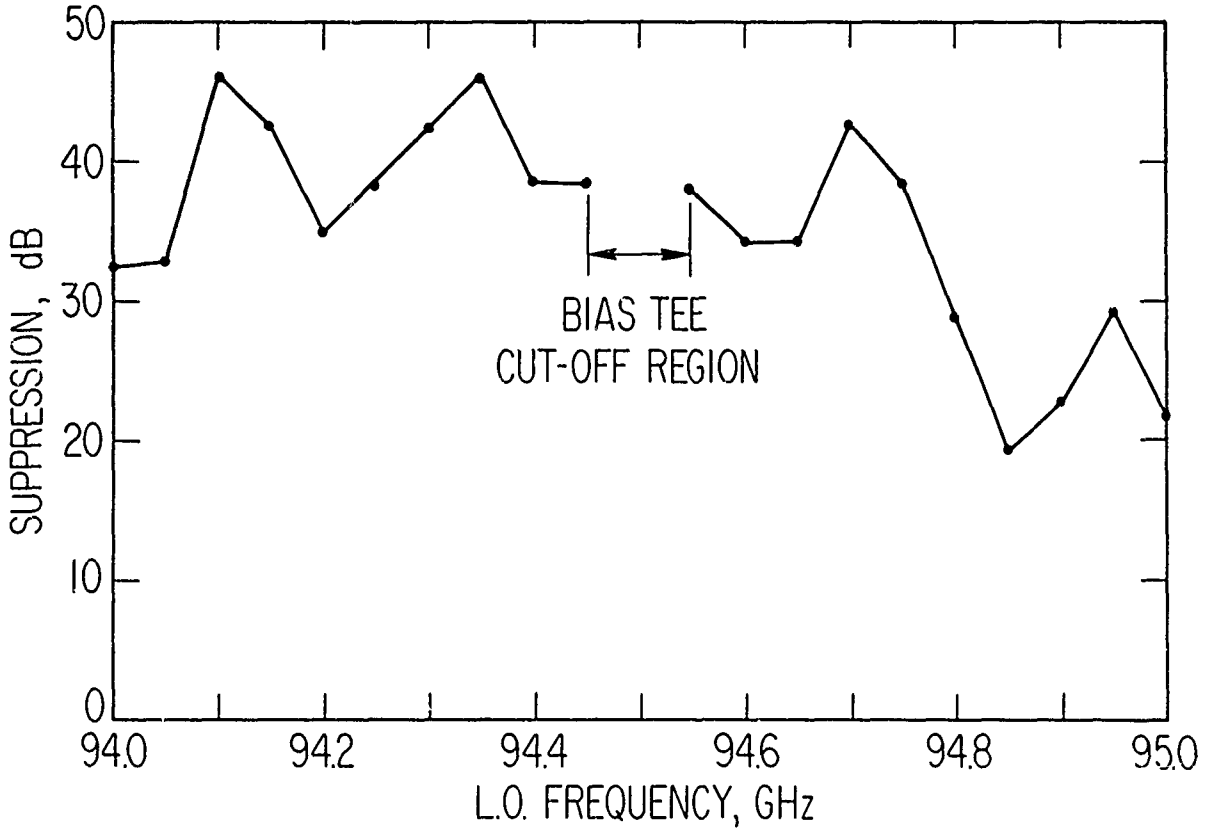

Figure 12. Calculated L. O. Suppression for Balanced Mixer Pair W-1 and W-2

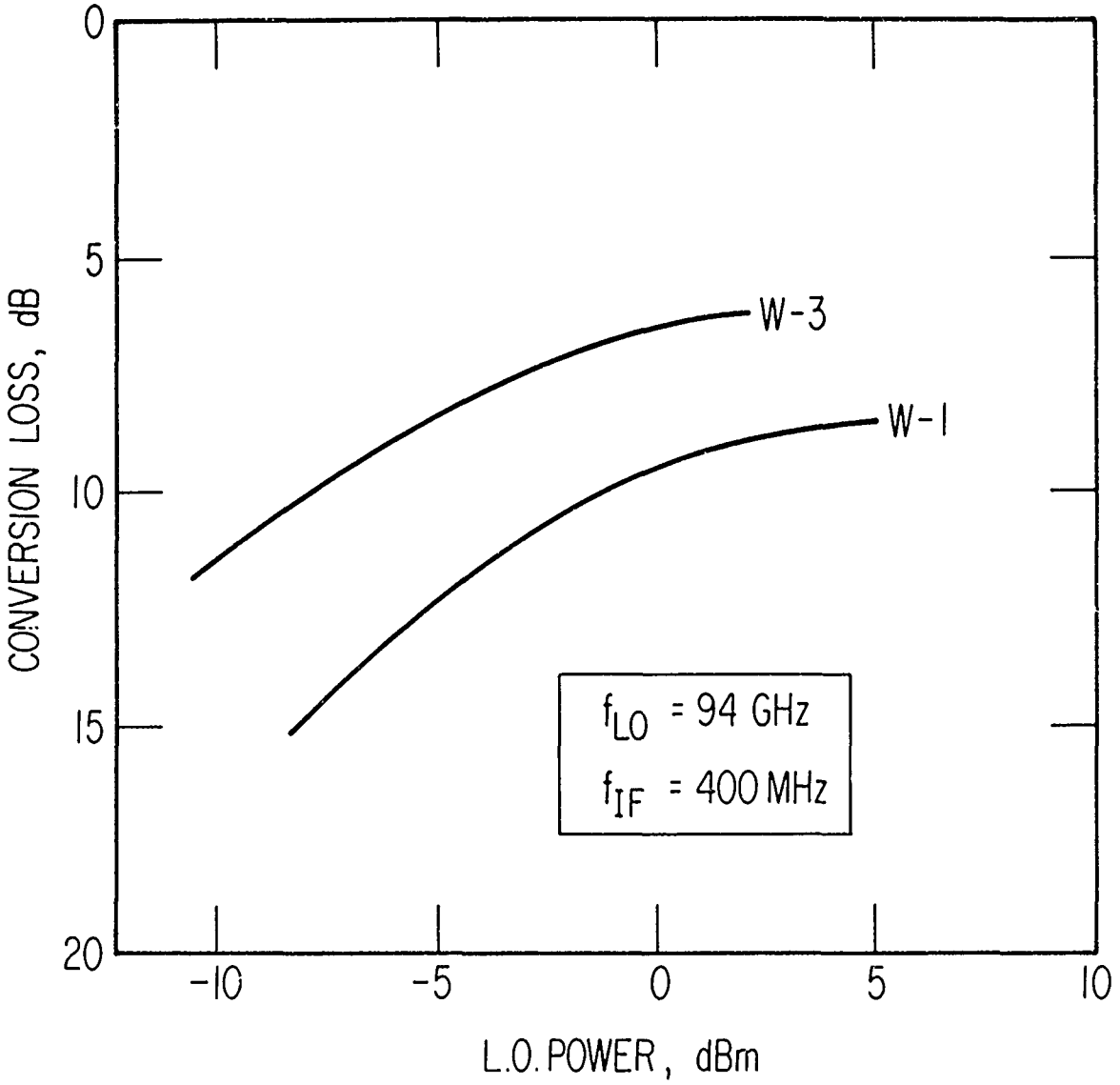

Figure 13. Conversion Loss vs L.O. Power for Diodes W-1 and W-3

Table I. Input VSWR vs Frequency

P_{LO} = 0 dBm, f_{LO} = 94.0 GHz, power in measurement signal = -13 dBm

Frequency	Input VSWR	
	Diode W-6	Diode W-7
91.0	2.30	2.10
92.0	1.80	1.80
93.0	1.60	1.65
93.5	1.50	1.75
94.0	1.25	1.70
94.5	1.30	1.60
95.0	1.20	1.35

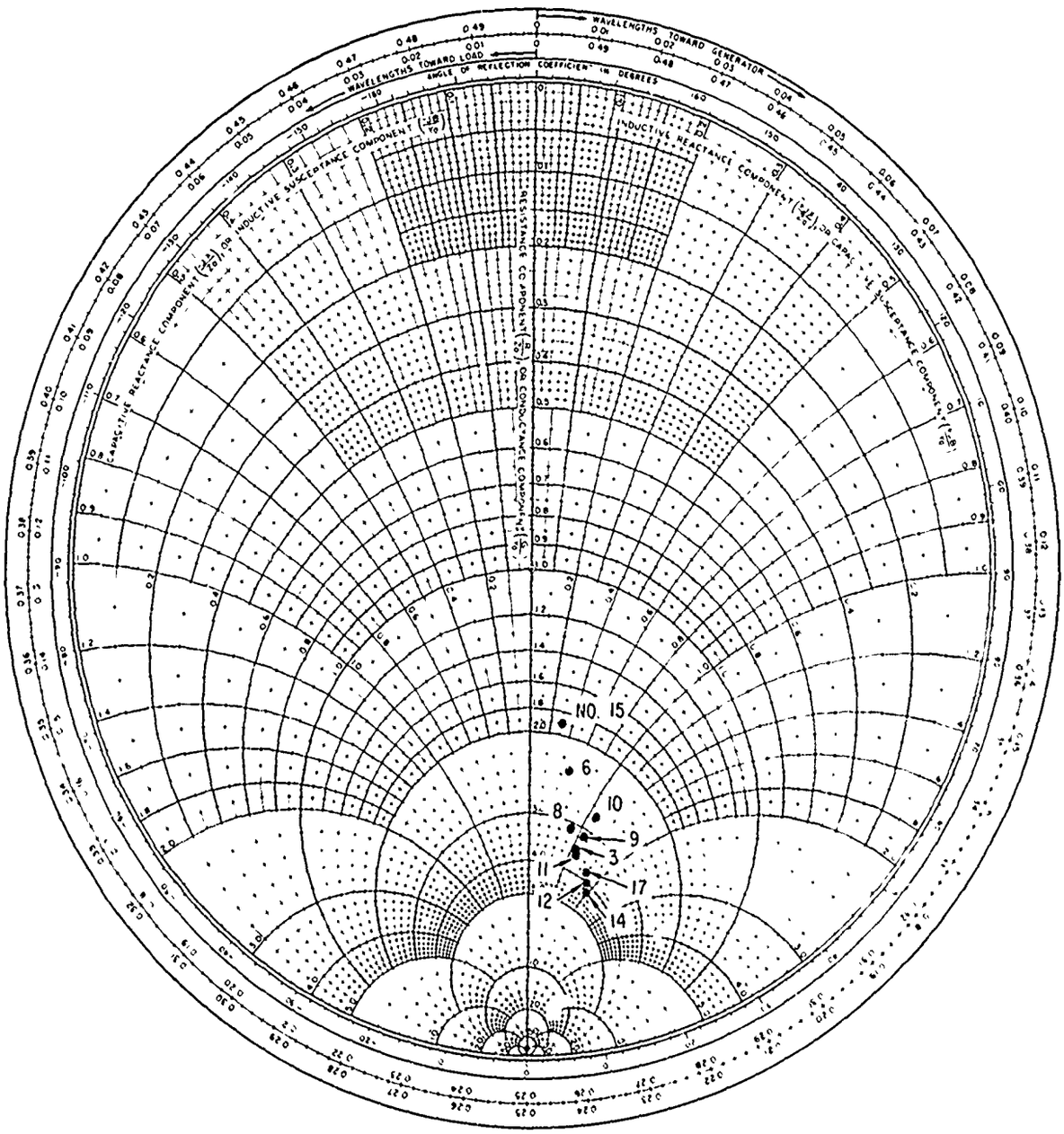

Figure 14. Diode Impedance at 125 MHz for Best Conversion Loss

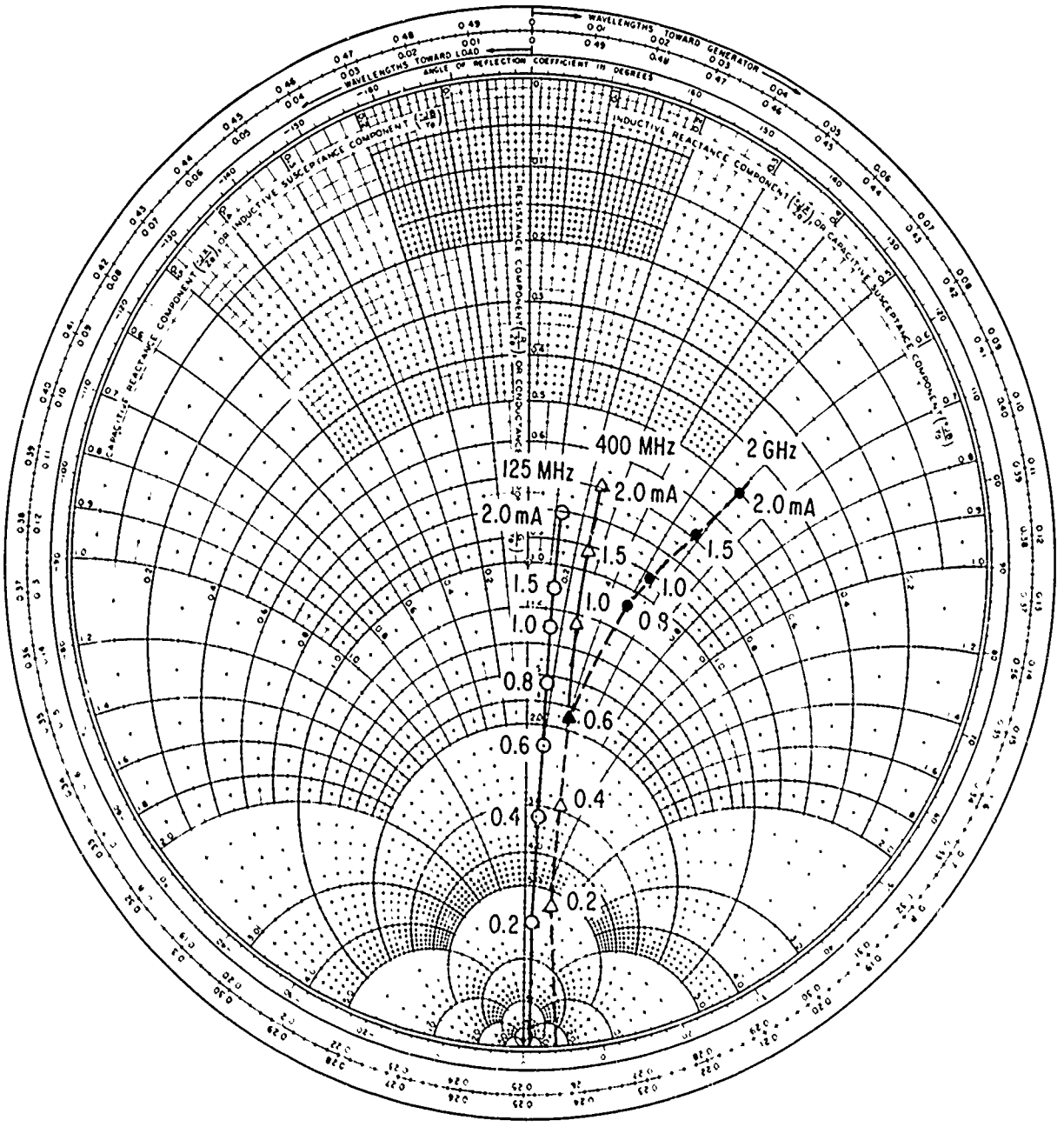

Figure 15. Impedance vs dc Current for Diode 3

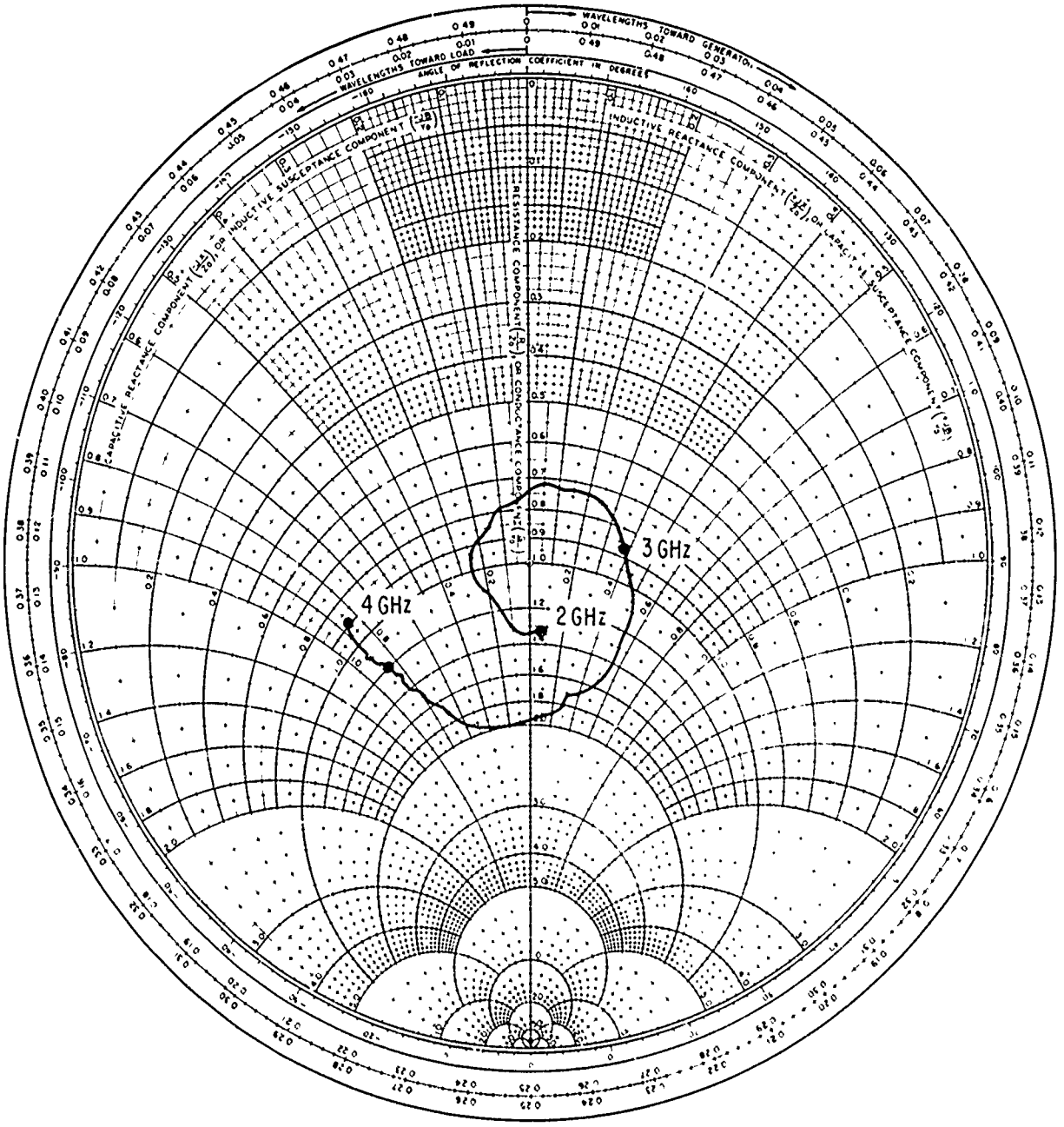

Figure 16. IF Impedance vs Frequency for Diode W-1 with 90-Ω Transformer

frequency, the IF impedance is higher when the diode is driven with RF than when it is not. Figure 16 is a plot of the IF impedance for mount No. W-1 with a 90-Ω quarter-wave transformer centered at 3 GHz to improve the IF match. From 2 to 4 GHz, the VSWR is less than 2.4:1. Without the matching network, the VSWR would have been greater than 3.0:1 over the same range.

IV. NOISE TEMPERATURE RATIO

A. GENERAL DISCUSSION

The noise temperature ratio t is defined as the ratio of the diode available noise power to that available from an ideal conductance of the same value of conductance as the diode. The noise properties of the diode can then be represented by the equivalent circuit of Figure 17.

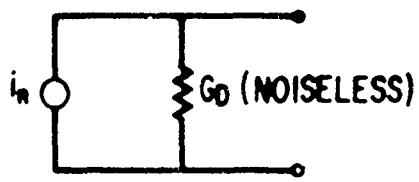

Figure 17. Noise Equivalent Circuit of Diode

In Figure 17, $\langle i_n^2 \rangle = 4kTBG_Dt$, where k = Boltzmann's constant = 1.38 $\times 10^{-23}$ j/°K, T = diode temperature in °K, B = bandwidth in Hz in which $\langle i_n^2 \rangle$ is measured, and G_D = diode conductance. Cowley and Zettler (Ref. 22) and Hsu (Ref. 27) have examined the noise properties of silicon Schottky barrier diodes both theoretically and in the laboratory. For a diode whose forward I-V characteristic is described by

$$I = I_{s0}(e^{qV/nkT} - 1) \tag{2}$$

where q is the electronic charge, I_{s0} is the saturation current, and n is the diode "ideality factor," normally slightly greater than unity, they predict a forward bias value of t of

$$t = \frac{n}{2}\left(1 + \frac{I_{s0}}{I + I_{s0}}\right) \tag{3}$$

Their derivation of Eq. (3) assumes full shot noise for the forward current I and for the equal and opposite saturation currents I_{s0} that flow in the barrier; i. e.,

$$\langle i_n^2 \rangle = 2q(I + 2I_{s0})B \tag{4}$$

Combining Eqs. (1), (2), and (4) and noting that $G_D = \partial I/\partial V$ gives the result in Eq. (3). The experimental work of Cowley and Zettler and Hsu shows excellent agreement with this theory when simple corrections are made for the thermal noise contribution of the diode series resistance. These authors further find that, at frequencies below a few kilohertz, the diodes exhibit noise in excess of that predicted; this noise has an approximate f^{-1} characteristic with a strong dependence on current, the noise generally increasing as the current is increased. Cowley and Sorenson (Ref. 28) compare the f^{-1} behavior of silicon point contact and Schottky barrier diodes and find that the Schottky barrier diodes give superior performance.

B. MEASUREMENTS

The measured noise temperature ratio t_m for representative diodes is plotted in Figures 18-23 for both frequency and current as the independent variable. The test procedures for obtaining these data are discussed in the Appendix. These data have a number of striking features. With reference to the t_m-vs-f curves, the t_m is relatively constant and very high at low frequencies and has a low-frequency corner at several hundred kilohertz, after which it decreases at a rate of $\sim f^{-2}$, with another corner frequency occurring at several hundred megahertz. From the t_m-vs-I_D curves, we see that below the lower corner frequency the value of t_m increases as I_D is increased from zero, reaches a peak, and then decreases with increasing I_D. For frequencies of several megahertz and above, the value of t_m generally increases as I_D is increased. Note also that the minimum value of t_m for all these diodes is

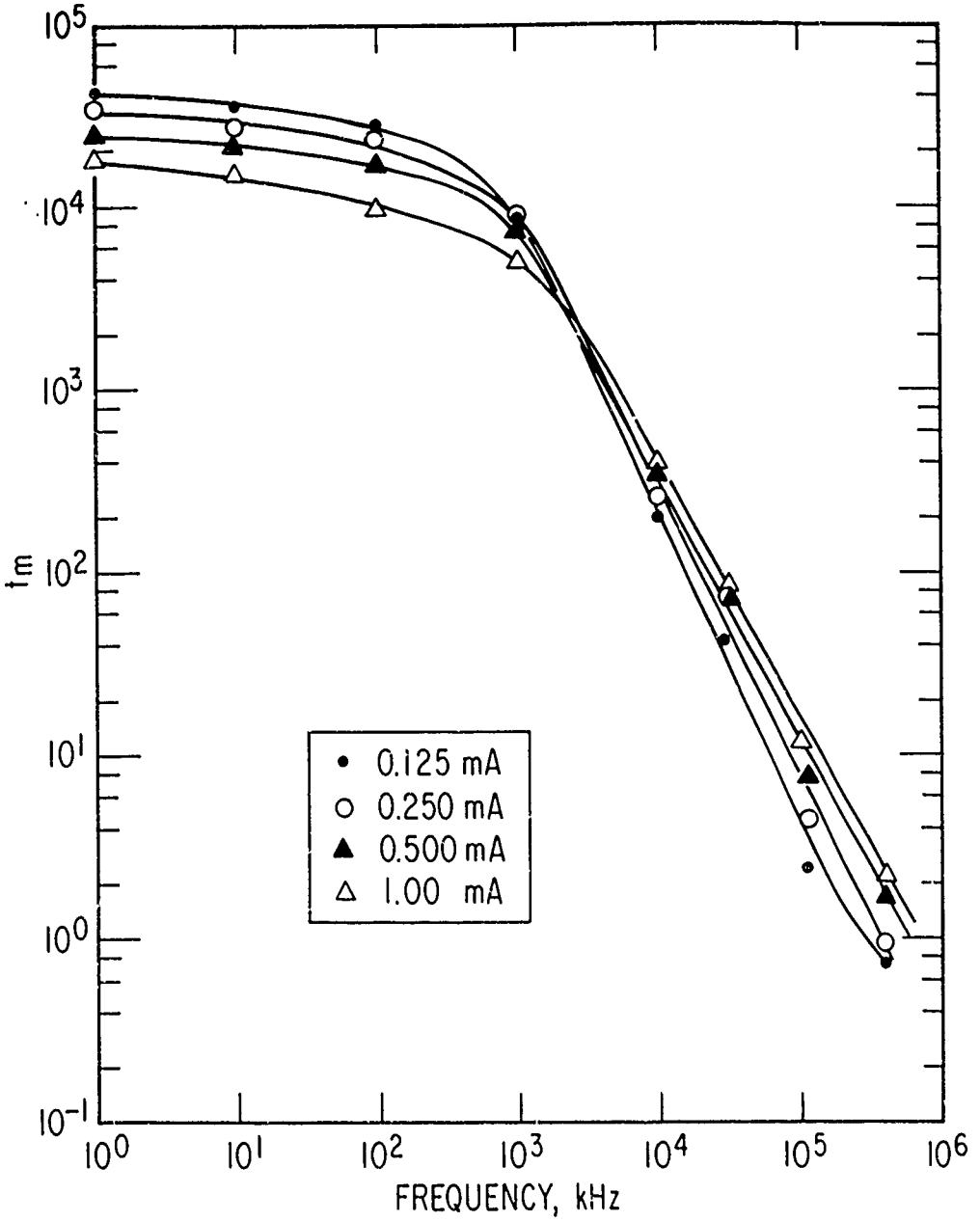

Figure 18. Measured Diode Excess Noise Ratio vs Frequency for Diode 3

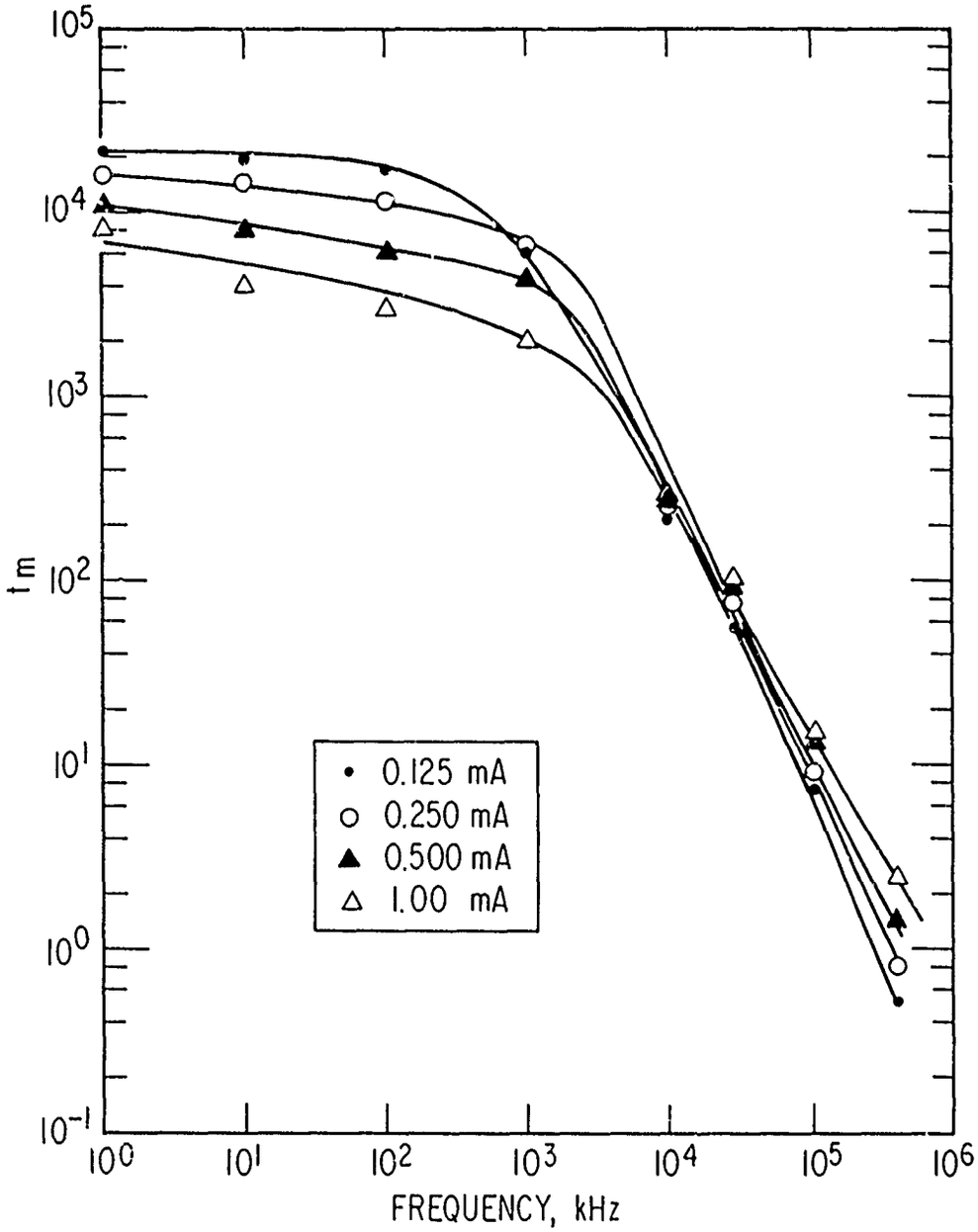

Figure 20. Measured Diode Excess Noise Ratio vs Frequency for Diode 8

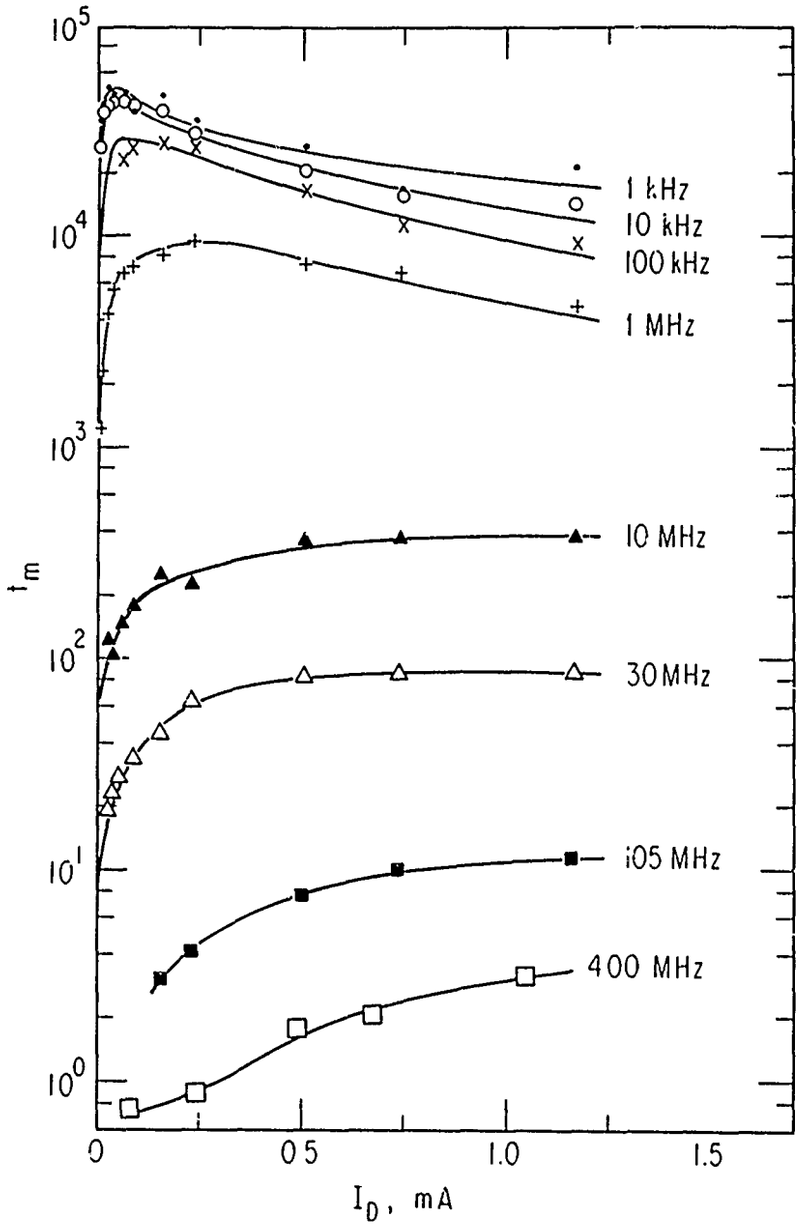

Figure 21. Measured Diode Excess Noise Ratio vs Current for Diode 3

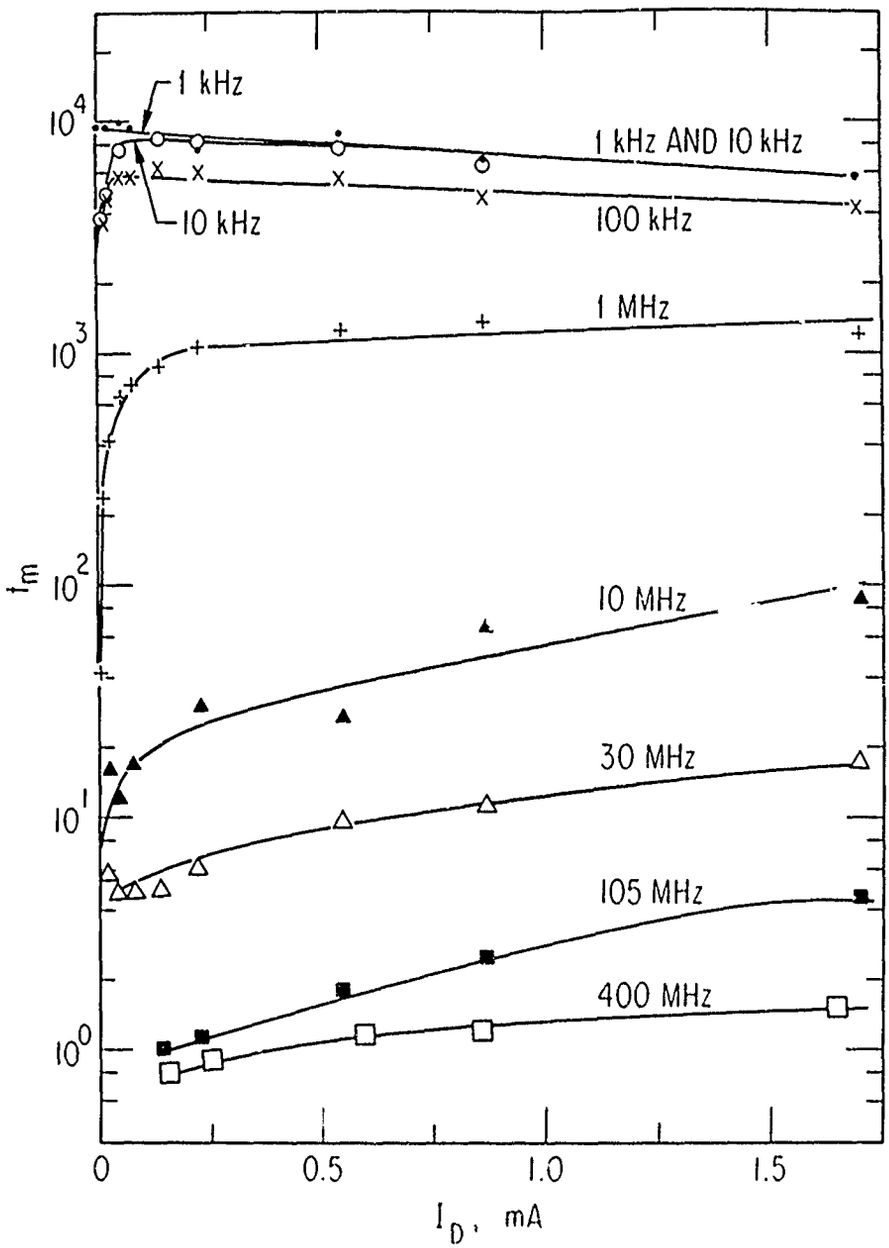

Figure 22. Measured Diode Excess Noise Ratio vs Current for Diode 6

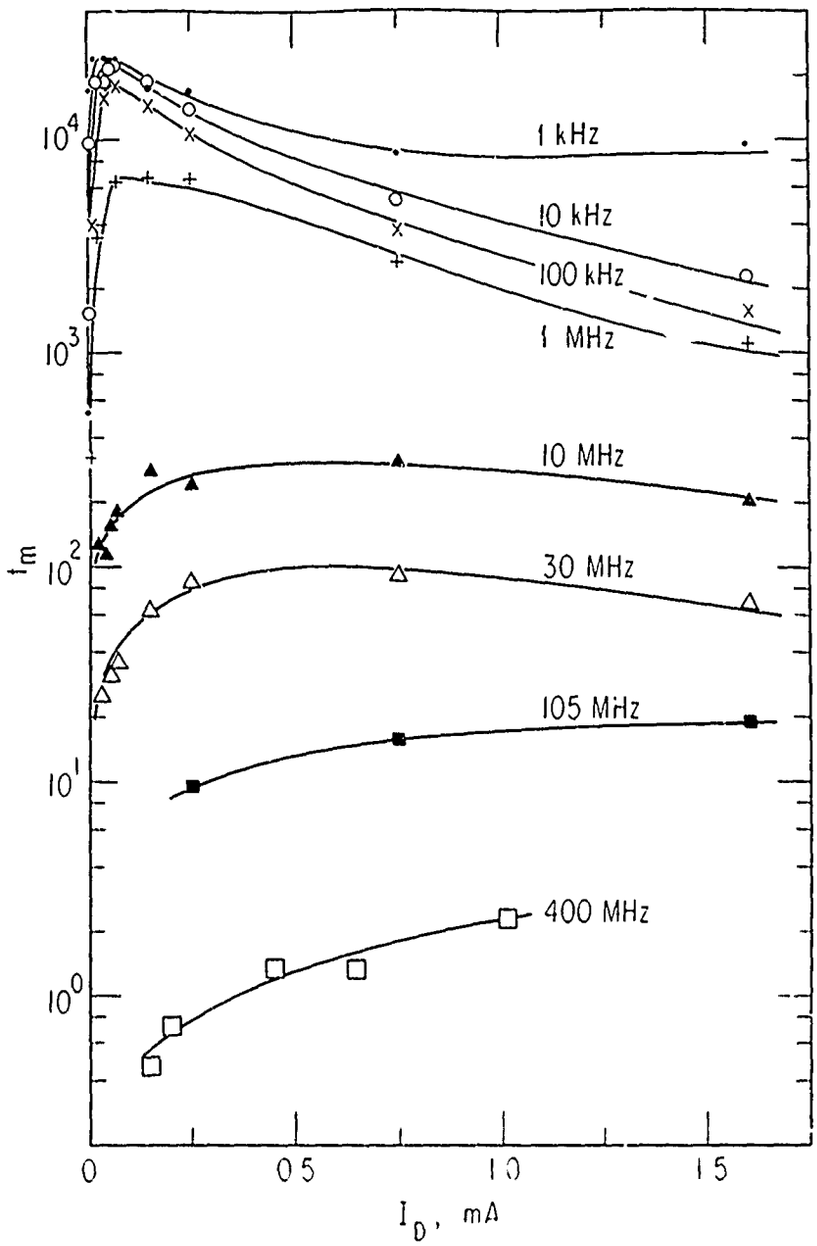

Figure 23. Measured Diode Excess Noise Ratio vs Current for Diode 8

less than unity. Since our ideality factors were close to unity and our saturation currents extremely small, this result is as expected, as can be seen from Eq. (3), which predicts a lower limit of 1/2 for t. The actual measured values of t, which we have called t_m, are somewhat different than the t predicted by Eq. (3) because of the diode series resistance R_S, which produces thermal noise independent of the noise of the Schottky barrier. The noise power per hertz P_D available between the diode terminals is therefore

$$P_D = \frac{tR_D + R_S}{R_D + R_S} kT \tag{5}$$

where $R_D = 1/G_D$. Then finally

$$t_m = \frac{tR_D + R_S}{R_D + R_S} \tag{6}$$

or

$$t = t_m + \frac{R_S}{R_D} (t_m - 1) \tag{7}$$

From Eq. (2) it is easily found that

$$G_D = \partial I/\partial V = \frac{q}{nkT} I_{s0} e^{qV/nkT} = \frac{q}{nkT} (I - I_{s0}) \sim \frac{q}{nkT} I \tag{8}$$

For example, at 290°K for n = 1 we would have

$$G_D \sim 40 \ I \tag{9}$$

Using Eqs. (7) and (9), along with the measured values of R_S and q/nkT and the values of t_m in Figures 18-20, we can compute t. The results, plotted vs frequency, are shown in Figures 24-26. Comparing these curves with those for t_m, we see that perhaps the only significant change is that, above the low-frequency corner, the values of t seem to be more linearly dependent on the bias current than was t_m. At present we have no straightforward theoretical explanation for the measured behavior. We are, however, still actively investigating the problem theoretically and through similar experimental measurements on diodes processed somewhat differently.

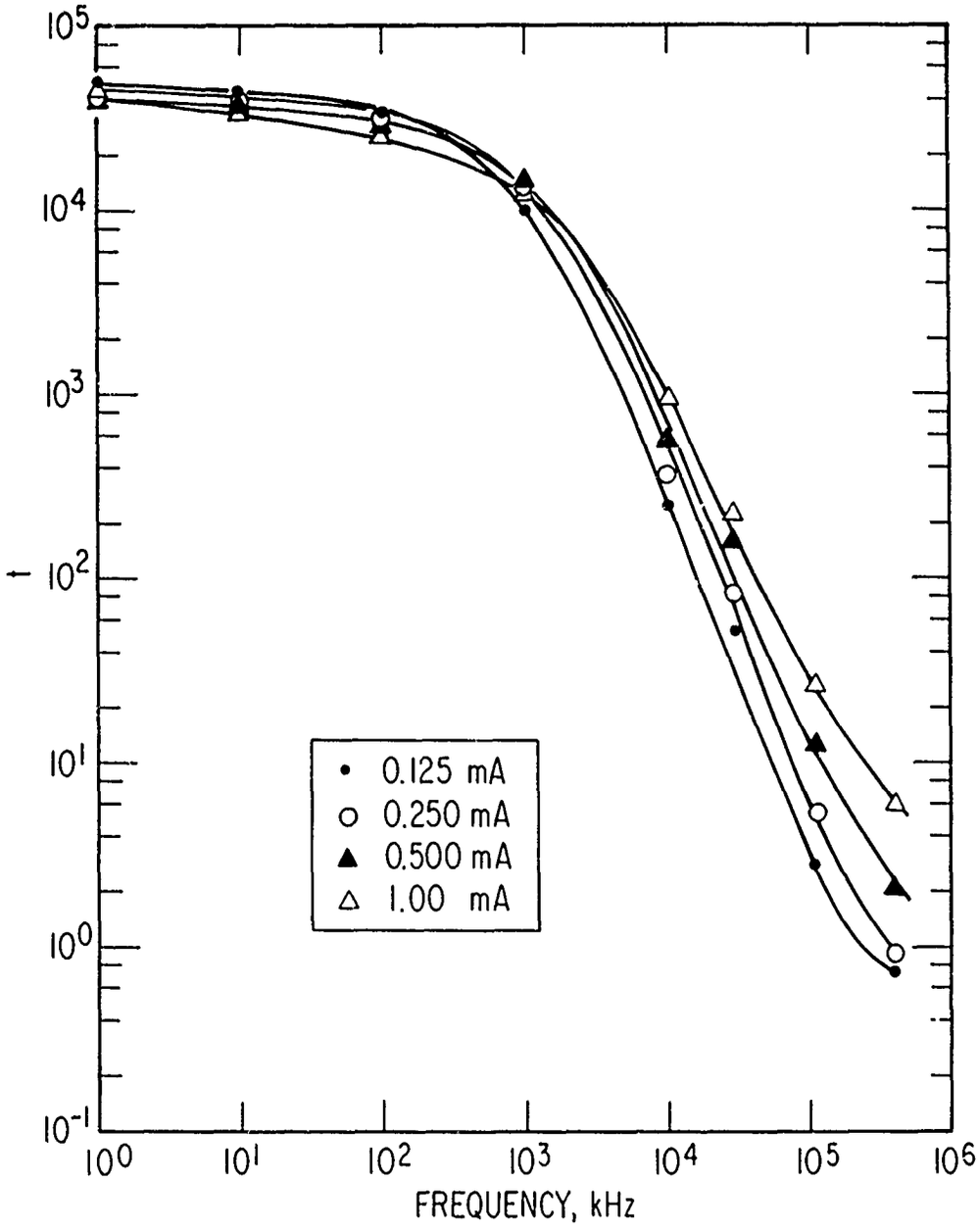

Figure 24. Computed Excess Noise Ratio of the Schottky Barrier as a Function of Frequency for Diode 3

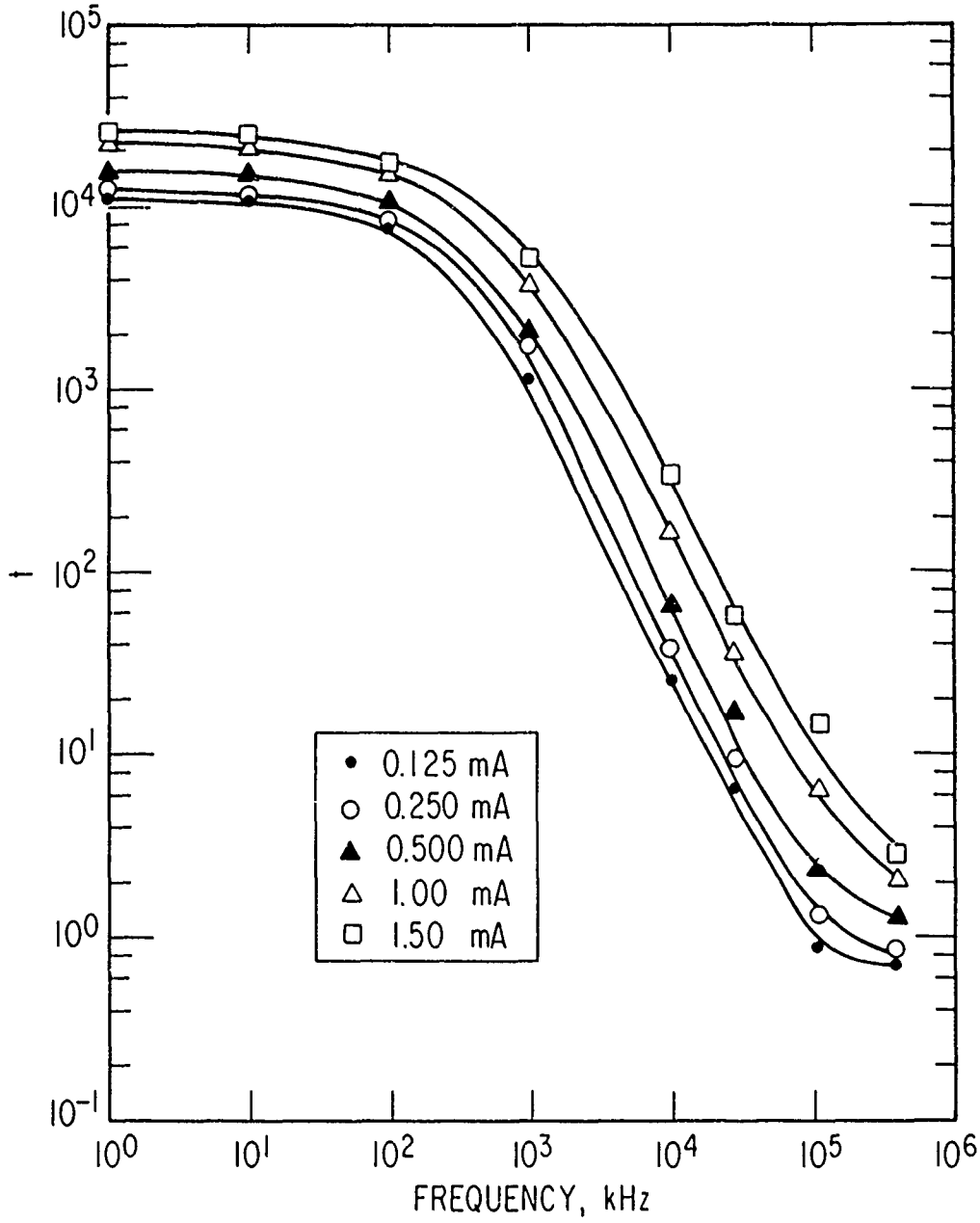

Figure 25. Computed Excess Noise Ratio of the Schottky Barrier as a Function of Frequency for Diode 6

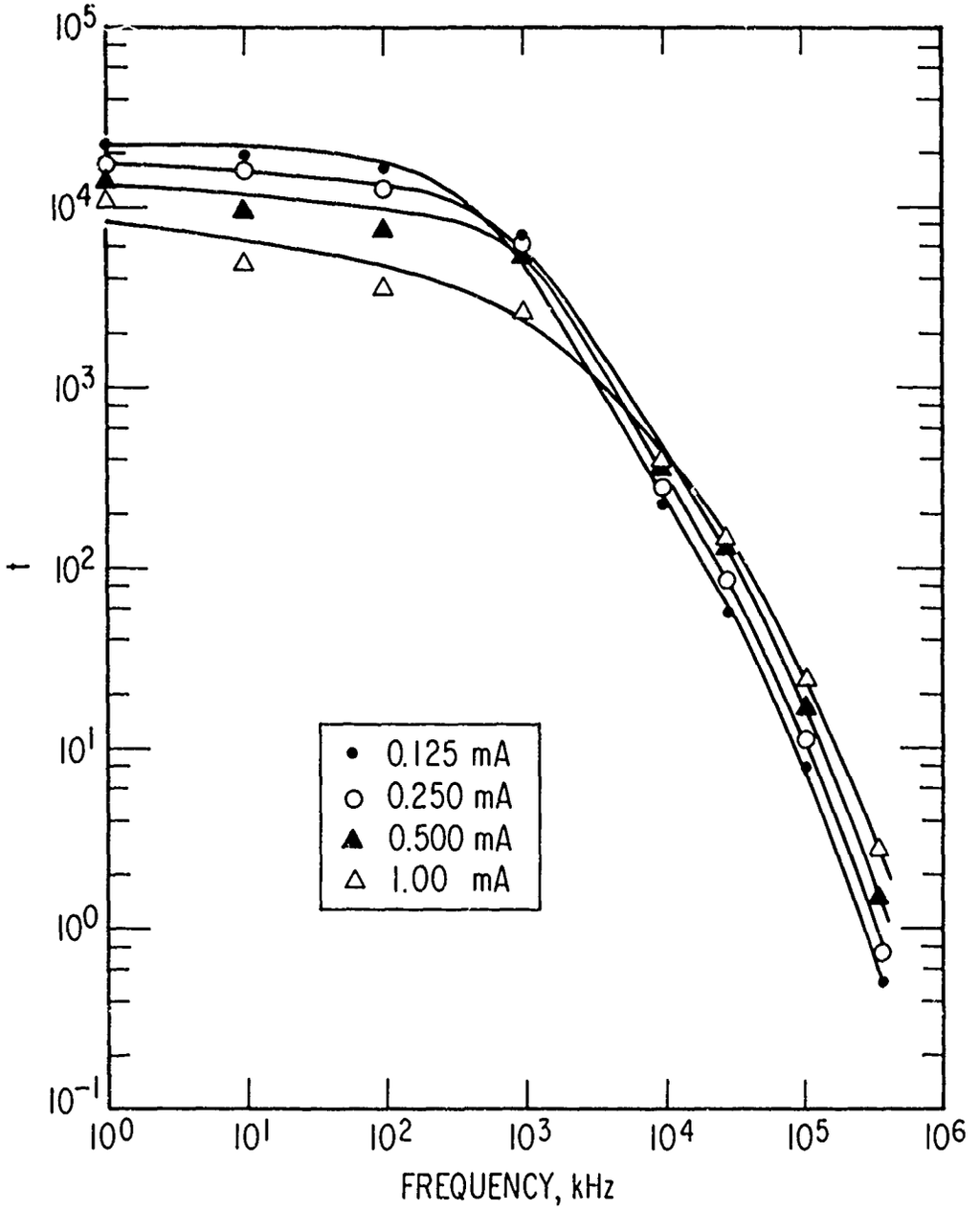

Figure 26. Computed Excess Noise Ratio of the Schottky Barrier as a Function of Frequency for Diode 8

V. NOISE FIGURE MEASUREMENTS

Noise figure measurements were made by the hot-cold body technique with a Signalite TN-111 gas tube. The temperature of the gas tube was established by comparison to ambient and liquid nitrogen loads with the use of a Dicke switched radiometer with an E and M Laboratories Model L 1020 1-2 GHz IF amplifier. Except for the IF, the radiometer is identical to that described by Johnson (Ref. 21). Two tubes were calibrated; the resulting temperatures were 10,300 and 12,000°K.

The noise figures of mixers No. W-4, No. W-7, and No. 17 were measured with the same 1-2 GHz amplifier used in the gas tube calibration. A tunnel diode detector was used to measure amplifier output power. The double sideband noise figures, including the amplifier contributions, were 8.6, 8.8, and 10.6 dB, respectively. We made a narrow band measurement at 1200 MHz on No. W-7 by following the 1-2 GHz amplifier with a 5-pole-pair filter with a 200-MHz, 3-dB bandwidth. This double sideband noise figure was measured to be 7.3 dB. Assuming that the sidebands are symmetrical then gives single sideband noise figures, which are 3 dB higher. Figure 27 shows the noise figure and gain characteristics of the IF amplifier as measured in a 50-Ω system. If an "average" noise figure of 3.5 dB is assumed for the amplifier, the sum of the conversion loss, the mixer excess noise, and the klystron noise contribution should be 8.1, 8.3, and 10.1 dB, respectively, for No. W-4, No. W-7, and No. 17 with the 1-2 GHz IF. Similarly, for the narrow-band measurement at 1200 MHz, the result should be 6.9 dB if we assume an amplifier noise figure of 3.4 dB at 1200 MHz. Since the amplifier was optimized for a 50-Ω system, these numbers are probably somewhat conservative.

The noise figure of the balanced mixer pair W-1 and W-2 was measured with a 200-500 MHz IF amplifier. With the gas tube calibration described above, the double sideband noise figure, including the amplifier figure, was 8.5 dB. Figure 28 shows the noise figure and gain characteristics of the IF

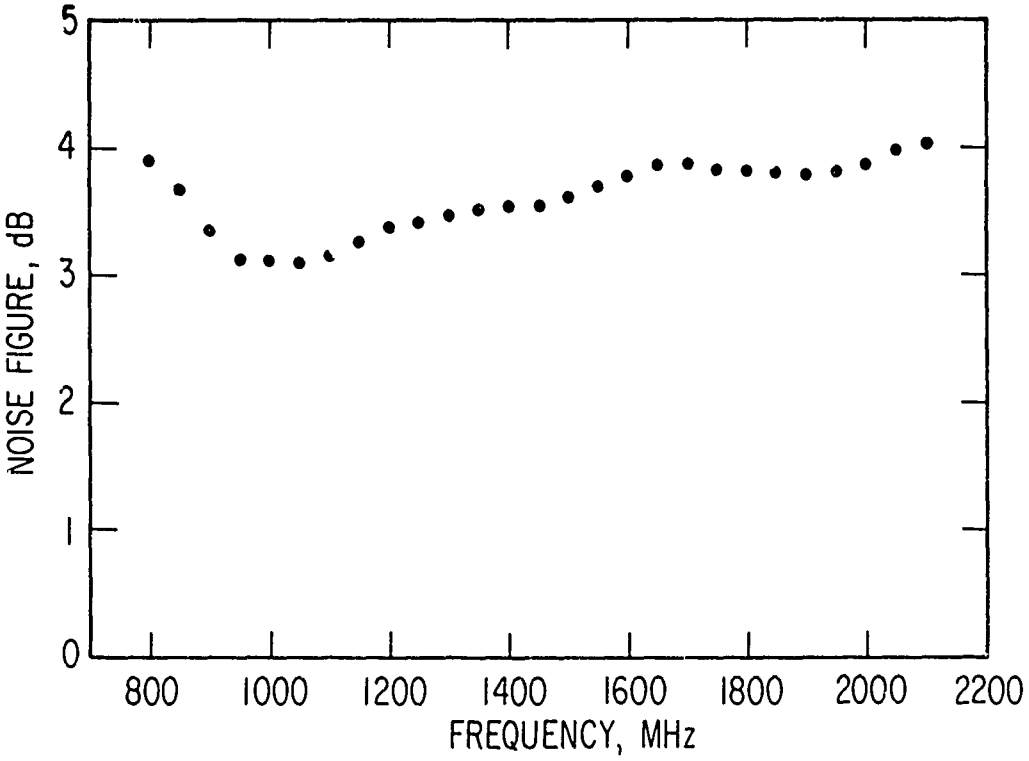

a. Noise Figure

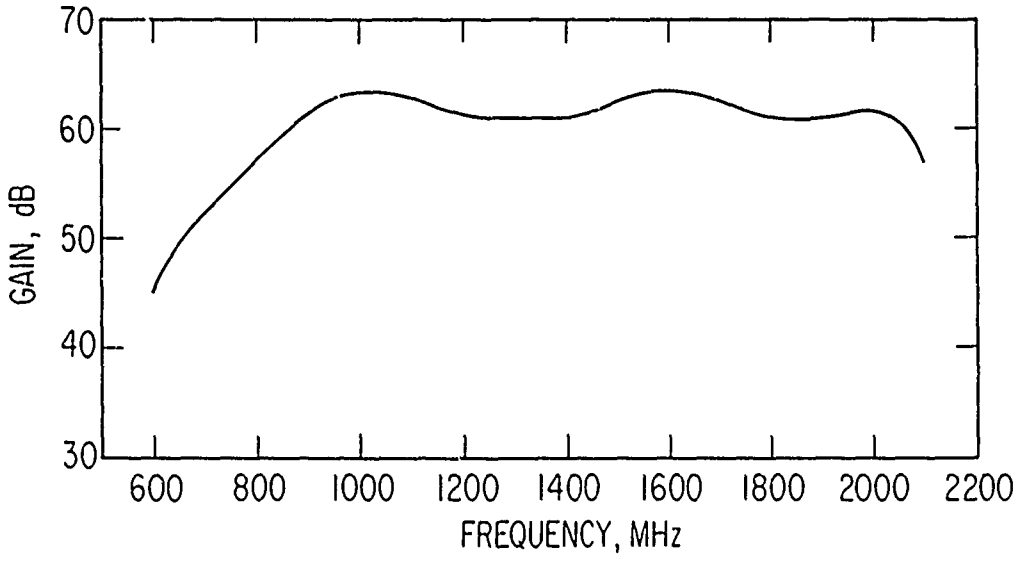

b. Gain

Figure 27. Noise Figure and Gain of E&M L-Band Amplifier vs Frequency

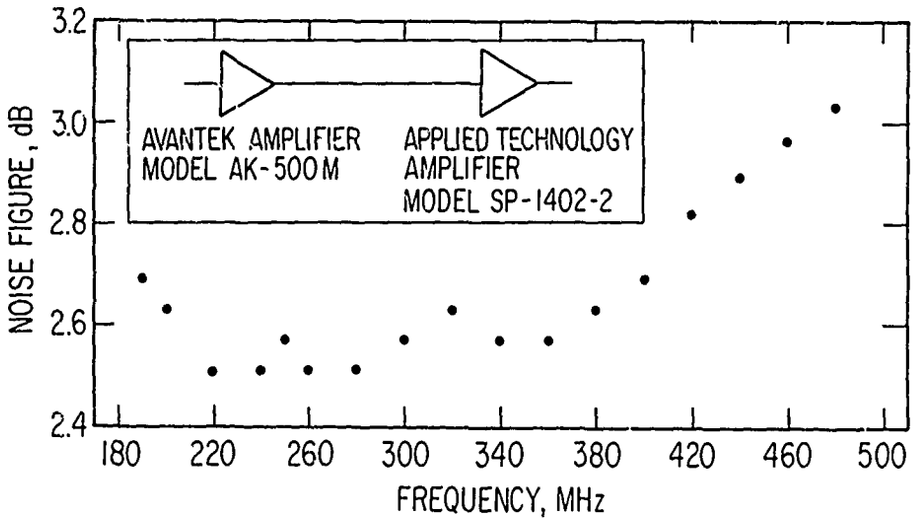

a. Noise Figure

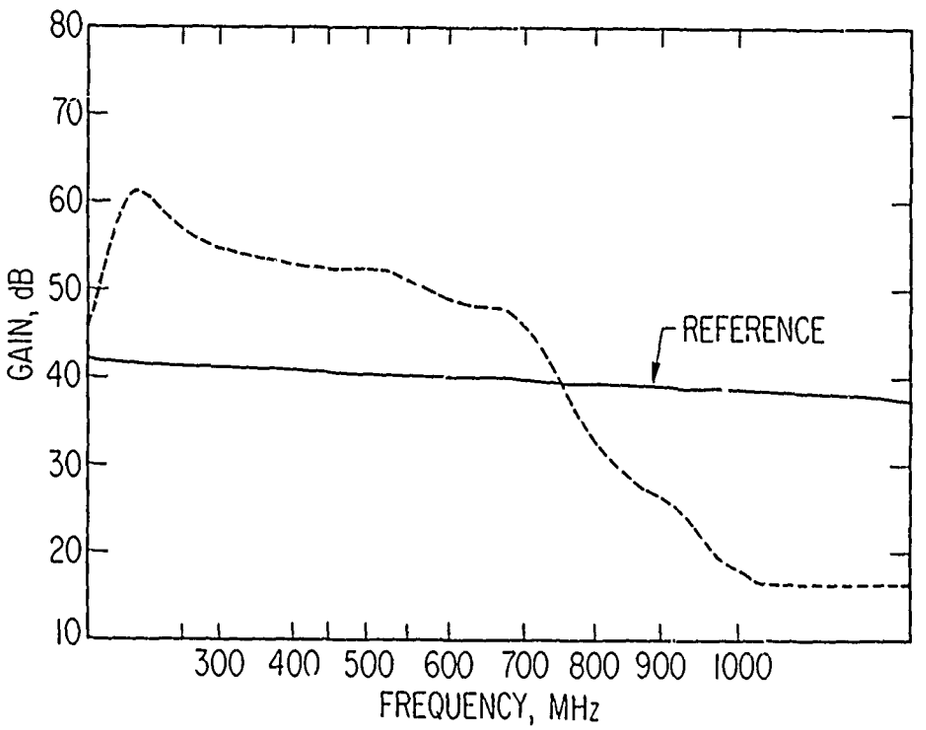

b. Gain

Figure 28. Noise Figure and Gain of Amplifier Pair vs Frequency

amplifier as measured in a 50-Ω system. If we assume an average IF noise figure of 2.6 dB, the sum of the conversion loss, the mixer excess noise, and the klystron noise is approximately 8.9 dB, again a somewhat conservative estimate.

In general, we find good agreement between noise figures predicted by our conversion and excess noise ratio measurements and those actually measured with the gas tube. The gas tube measurement is, however, certainly the more accurate of the two methods.

VI. CONCLUSIONS

Data have been presented that show the conversion and excess noise ratio characteristics of 3.3-mm GaAs Schottky barrier mixers. It is possible to achieve a conversion loss of 5 dB, although a loss of 7-10 dB is more common. A bandwidth of 8.6 GHz for a variation of ±0.7 dB was demonstrated. The upper-corner frequency for the diode excess noise ratio is on the order of several hundred megahertz, and asymptotic values of less than unity were achieved. The dependence with frequency is f^{-2} with a lower-corner frequency of several hundred kilohertz, below which the curves are relatively flat to at least 1 kHz, the lowest frequency of measurement. The relatively noisy nature of these diodes at low frequencies precludes their use in low-IF systems but would be of no consequence for IF's above several hundred megahertz. These unusual noise properties result from the addition of the Cu impurity in the GaAs processing.

The design of a new and more rugged mixer mount is presented and the technique of making diode contacts in the mount discussed. It is shown that improved RF matching characteristics of the diodes result from the Cu impurity doping. The characteristics of a balanced mixer with a pair of these mounts is shown.

The results of noise figure measurements made by use of a hot-cold body technique are given for single-ended mixers with a 1-2 GHz IF. The double sideband noise figures are 8.6, 8.8, and 10.6 dB. A narrow-band measurement for a 1.2-GHz IF and a single-ended mixer shows that a double sideband noise figure of 7.3 dB is possible. Use of 200-500 MHz IF following a balanced mixer results in a double sideband noise figure of 8.5 dB.

REFERENCES

1. M. Cohn and L.E. Dickens, "Recent developments in millimeter wave components," 1969 G-MTT Intern. Microwave Symp. Digest, pp. 225-229 (1969).

2. J. Edrich, "A parametric amplifier for 46 GHz," Proc. IEEE (Lett.), vol. 59, no. 7, pp. 1125-1126 (July 1971).

3. G. D. Messenger and C. T. McCoy, "Theory and operation of crystal diodes as mixers," Proc. IRE, vol. 45, no. 9, pp. 1269-1283 (September 1957).

4. C. T. McCoy, "Present and future capabilities of microwave crystal receivers," Proc. IRE, vol. 46, no. 1, pp. 61-66 (January 1958).

5. D. A. Jenny, "A gallium arsenide microwave diode," Proc. IRE, vol. 46, no. 4, pp. 717-722 (April 1958).

6. W. M. Sharpless, "Wafer-type millimeter wave rectifiers," Bell System Tech. J. vol. 35, 1956, pp. 1385-1402 (November 1956).

7. W. M. Sharpless, "Point-contact wafer diodes for use in the 90- to 140-kilomegacycle frequency range," Bell System Tech. J. vol. 42, pp. 2496-2499 (September 1963).

8. C.A. Burrus, "Backward diodes for low level millimeter-wave detection," IEEE Trans. Microwave Theory Tech., vol. MTT-11, pp. 357-362 (September 1963).

9. R. Meredith and F. L. Warner, "Superheterodyne radiometers for use at 70 Gc and 140 Gc," IEEE Trans. Microwave Theory Tech., vol. MTT-11, pp. 397-411 (September 1963).

10. W. M. Sharpless, "Gallium-arsenide point-contact diodes," IRE Trans. Microwave Theory Tech., vol. MTT-9, pp. 6-10 (January 1961).

11. M. McColl, M. F. Millea, J. Munushian, and D. F. Kyser, "Improved 94 GHz GaAs mixer diodes using gold-copper alloy whiskers," Proc. IEEE (Lett.), vol. 55, no. 12, pp. 2169-2170 (December 1967).

Preceding page blank

REFERENCES (Continued)

12. J. W. Dees, "Detection and harmonic generation in the submillimeter wavelength region," Microwave J., vol. 9, no. 9, pp. 48-55 (September 1966).

13. L. E. Dickens, J. M. Cotton, and B. D. Geller, "A mixer and solid state L.O. for a 60 GHz receiver," 1971 G-MTT Intern. Microwave Symp. Digest, pp. 188-190 (1971).

14. D. T. Young and J. C. Irvin, "Millimeter frequency conversion using Au-n-type GaAs Schottky barrier epitaxial diodes with a novel contacting technique," Proc. IEEE (Lett.), vol. 53, no. 12, pp. 2130-2131 (December 1965).

15. W. V. T. Rusch and C. A. Burrus, "Planar millimeter-wave epitaxial silicon Schottky-barrier converter diodes," Solid-State Electron., vol. 11, no. 5, pp. 517-525 (May 1968).

16. M. Cohn, F. L. Wentworth, and J.C. Wiltse, "High sensitivity 100- to 300-Gc radiometers," Proc. IEEE, vol. 51, no. 9, pp. 1227-1232 (September 1963).

17. R. J. Bauer, M. Cohn, J. M. Cotton, and R. F. Packard, "Millimeter wave semiconductor diode detectors, mixers, and frequency multipliers," Proc. IEEE, vol. 54, no. 4, pp. 595-605 (April 1966).

18. C. A. Burrus, "Millimeter-wave point-contact and junction diodes," Proc. IEEE, vol. 54, no. 4, pp. 575-587 (April 1966).

19. M. F. Millea, M. McColl, and C. A. Mead, "Schottky barriers on GaAs," Phys. Rev., vol. 177, no. 1, pp. 1164-1172 (January 1969).

20. F. L. Wentworth, J. W. Dozier, and J. D. Rodgers, "Millimeter wave harmonic generators, mixers and detectors," Microwave J., vol 7, no. 6, pp. 69-75 (June 1964).

21. W. A. Johnson, "Performance of a 3.3-mm radiometer," IEEE Trans. Microwave Theory Tech., vol. MTT-16, no. 9, pp. 621-625 (September 1968).

22. A. M. Cowley and R. A. Zettler, "Shot noise in silicon Schottky barrier diodes," IEEE Trans. Electron. Devices, vol. ED-15, no. 10, pp. 761-769 (October 1968).

23. L. A. Hoffman, D. E. Kind, and H. J. Wintroub, Large Time-Bandwidth Product Modulation Experiments at 94 GHz, TR-0158(3230-46)-3, The Aerospace Corp., El Segundo, Calif. (September 1967).

24. W. A. Johnson, Stability, Linearity, and Optimization of the Linear FM Sweep Generation Loop for a 3.2-mm Radar, TR-0172(2230-20)-8, The Aerospace Corp., El Segundo, Calif. (August 1971).

25. L. A. Hoffman, K. H. Hurlbut, D. E. Kind, and H. J. Wintroub, "A 94-Gc radar for space object identification," IEEE Trans. Microwave Theory Tech., vol. MTT-17, pp. 1145-1149 (December 1969).

26. R. V. Pound, Microwave Mixers, New York: McGraw-Hill, 1948, pp. 273-274.

27. S. T. Hsu, "Low-frequency excess noise in metal silicon Schottky barrier diodes," IEEE Trans. Electron. Devices, vol. ED-17, no. 7, pp. 496-506 (July 1970).

28. A. M. Cowley and H. O. Sorensen, "Quantitative comparison of solid-state microwave detectors," IEEE Trans. Microwave Theory Tech., vol. MTT-14, no. 12, pp. 588-602 (December 1966).

29. H. A. Haus et al., "IRE standards on methods of measuring noise in linear twoports, 1959," Proc. IEEE, vol. 48, no. 1, pp. 60-68 (January 1960).

APPENDIX. MEASUREMENT OF NOISE TEMPERATURE RATIO t_m

An amplifier with noise N, gain G, and input and output impedances Z_i and Z_o, respectively, can be represented as in Figure A-1,

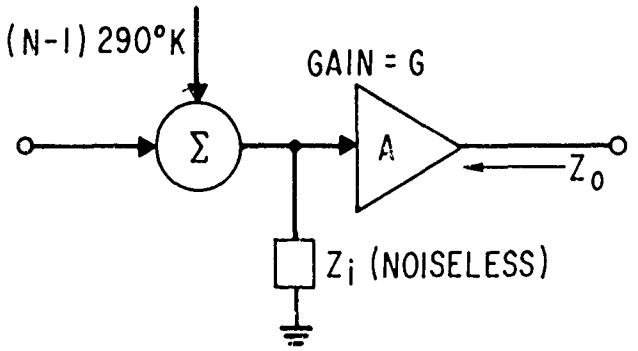

Figure A-1. Amplifier Equivalent Circuit

where A is now a noiseless amplifier whose gain and impedance characteristics are identical to those of the actual amplifier. The noise of the actual amplifier is represented by the added temperature (N - 1) 290°K, which is, of course, the amplifier "effective noise temperature" (Ref. 29). In general, N, G, Z_i, and Z_o are functions of frequency, and N may also be strongly dependent on the impedance of whatever source is connected to the amplifier input. If we now connect an ideal conductance G (generating only thermal noise) at temperature T_A to the amplifier input, the output power P_{o1} is given by

$$P_{o1} = [kT_A + k(N - 1)290]G \qquad (A-1)$$

Preceding page blank

If the ideal conductance is now replaced by a diode of the same conductance G at temperature T_A with a noise temperature ratio t_m, the output power P_{o2} is given by

$$P_{o2} = [Kt_m T_A + K(N - 1)290]G \tag{A-2}$$

and

$$\frac{P_{o2}}{P_{o1}} = \frac{t_m T_A + (N - 1)290}{T_A + (N - 1)290} \tag{A-3}$$

If the measurements are made at laboratory ambient temperature (approximately 294°K) as the reference in which case

$$\frac{P_{o2}}{P_{o1}} \approx \frac{t_m + N - 1}{N} \tag{A-4}$$

and

$$t_m = 1 + N\left(\frac{P_{o2}}{P_{o1}} - 1\right) \tag{A-5}$$

Therefore, for measurement of the t_m at 10 kHz, for example, a 10-kHz low-noise, narrowband, high-gain amplifier is constructed, the noise figure is measured as a function of the driving impedance, and P_{o1} and P_{o2} are measured with a true rms voltmeter. Equation (A-5) is then used to compute t_m. For the measurements reported in this paper, amplifiers were constructed at 1, 10, and 100 kHz and 1, 10, 30, 105, and 400 MHz. The amplifier noise outputs (P_{o1} and P_{o2}) are measured directly with a Ballantine 320A true rms voltmeter for the 1, 10, and 100 kHz and 1 MHz cases. For the 10, 30, 105, and 400 MHz cases, a mixer is employed as shown in Figure A-2.

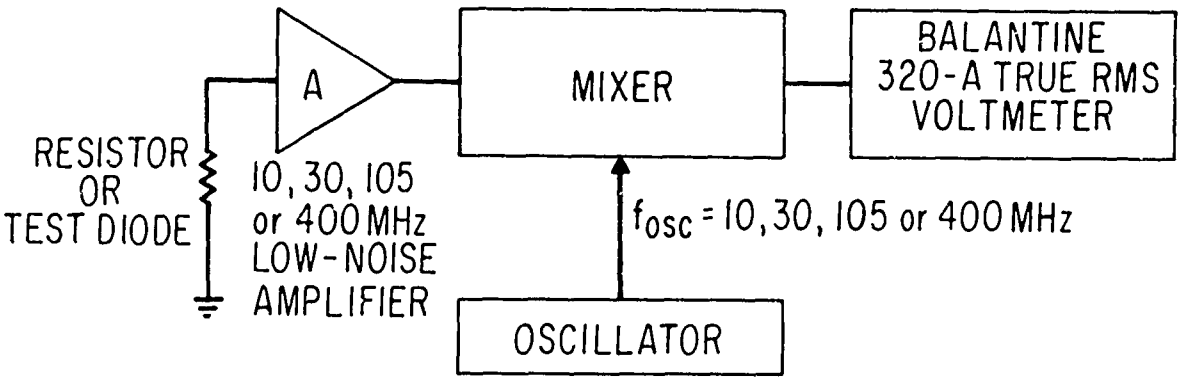

Figure A-2. Noise Measurement Test Configuration

Amplifier noise figure is measured with a hot-cold body technique, which involves (1) terminating the amplifier input with a precision film resistor at laboratory ambient temperature and measuring the amplifier power output and (2) cooling the termination to liquid nitrogen temperature (77.3°K). The amplifier noise figure can then easily be computed. A typical curve of noise figure vs termination resistance is shown in Figure A-3. For the 30, 105, and 400 MHz measurements, the noise figure is measured with precisely the same line length as is employed when the diode noise is measured. This line length (~5 in.) is measured by means of an impedance measurement of the cable and diode mount with an open-circuited diode in the mount.

We see from Eq. (5) that the errors in t_m depend upon both the magnitudes, and the uncertainties in the measurements of, the quantities P_{o2}/P_{o1} and N. The quantity N also depends on a power ratio measurement. The absolute accuracy of voltage measurement on the Ballantine 320A voltmeter varies somewhat with voltage magnitude and frequency but is on the order of a few percent. Voltage ratios, however, should be much more accurate (particularly if they are close to unity) and are probably limited only by how well the observer can read the instrument. For many of the measurements

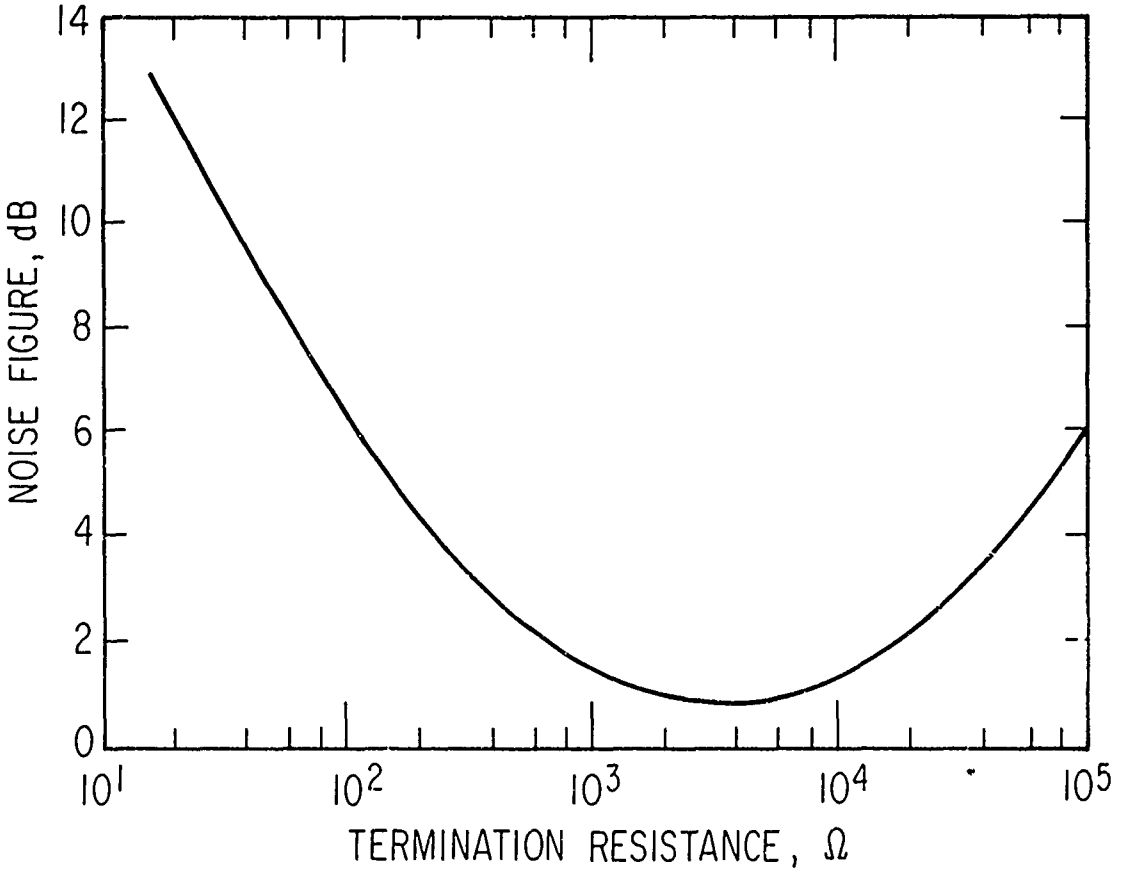

A-3. Noise Figure of 10-kHz Amplifier

a recorder or an integrating digital voltmeter is used on the Ballantine output to further improve the measurement accuracy. For the majority of the measurements reported here, the range of N is between 1.2 and 5, with errors of a few percent at the low end to perhaps ten percent at the high end. In general, then, our overall errors should be between a few percent and perhaps fifteen percent; the errors are generally smaller for the smaller values of t_m.